2016

IN VITRO VISUALIZATION OF PEDIATRIC SIZED MECHANICAL HEART VALVE PERFORMANCE USING AORTIC ROOT MODEL IN MOCK CIRCULATORY LOOP

Sarah Lederer
bradysl@vcu.edu

IN VITRO VISUALIZATION OF PEDIATRIC SIZED MECHANICAL HEART VALVE PERFORMANCE USING AORTIC ROOT MODEL IN MOCK CIRCULATORY LOOP

A thesis submitted in partial fulfillment of the requirements for the degree of Master of Science in Biomedical Engineering at Virginia Commonwealth University.

By

Sarah Brady Lederer

B.S. in Engineering

East Carolina University, 2014

Director: Gerald E. Miller, Ph.D.

Professor, Department of Biomedical Engineering

Director, Center for Human Factors and Rehabilitation Engineering

Virginia Commonwealth University

Richmond, Virginia

May 2016

ACKNOWLEDGEMENTS

I would first like to thank my faculty advisor Dr. Gerald Miller for the opportunity to work in the Artificial Heart Laboratory the past two years and for his support and guidance throughout my research. The skills and experiences gained by working in this laboratory will prove extremely useful as I begin my career as an engineer, and for that I am very grateful. I would also like to thank Dr. Ding-Yu Fei and Dr. James Arrowood for serving as members on my advisory committee and taking the time to review my work.

I would also like to express my gratitude for my fellow lab partner, Kayla Moody. I am proud to say I started and ended my time in the VCU biomedical engineering program alongside such a helpful, knowledgeable, and caring person. Without your tremendous help in the laboratory my thesis work would have proven quite difficult. In addition, I would also like to thank the rest of my fellow graduate BME colleagues for their contribution to my positive experience here in Richmond.

Finally, I would be remiss if I did not thank both my family and friends for their support and encouragement throughout my educational endeavors. My husband Drew, your unwavering support of me choosing to continue my education means the world to me and I couldn't have done it without you encouraging me along the way.

TABLE OF CONTENTS

LIST OF TABLES

LIST OF FIGURES

ABSTRACT

IN VITRO VISUALIZATION OF PEDIATRIC SIZED MECHANICAL HEART VALVE PERFORMANCE USING AORTIC ROOT MODEL IN MOCK CIRCULATORY LOOP

By Sarah Brady Lederer, B.S. in Engineering

A thesis submitted in partial fulfillment of the requirements for the degree of Master of Science in Biomedical Engineering at Virginia Commonwealth University.

Virginia Commonwealth University, 2016

Director: Gerald E. Miller, Ph.D.

Professor, Biomedical Engineering

Congenital heart valve disease is one of the most common abnormalities in children, with common valve defects being aortic stenosis, mitral stenosis, and valvular regurgitation. Although adult sized mechanical heart valve (MHV) replacements are widely studied and utilized, there are currently no FDA approved prosthetic heart valves available for the pediatric population. This is due to a variety of reasons such as a limited patient pool for clinical trials, limited valve sizes, and complex health histories in children. Much like adult sized mechanical heart valves, potential complications with pediatric heart valve replacements include thrombosis, blood damage due to high shear stresses, and cavitation. Due to pediatric sized MHVs being much smaller in size than adult MHVs, different fluid dynamic conditions and associated complications are expected. In order to accelerate the approval of pediatric sized heart valves for clinical use, it is important to first characterize and assess the fluid dynamics across pediatric sized heart valves. By understanding the hemodynamic performance of the valve, connections can be made concerning potential valve complications such as thrombosis and cavitation. The

overall objective of this study is to better characterize and assess the flow field characteristics of a pediatric sized mechanical heart valve using flow visualization techniques in a mock circulatory loop. The mechanical heart valve chosen for this research was a size 17 mm Bjork-Shiley tilting disc valve, as this is a common size valve used for younger patients with smaller cardiovascular anatomy. The mock circulatory loop used in this research was designed to provide realistic pediatric physiological flow conditions, consisting of a Harvard Apparatus Pulsatile blood pump, venous reservoir, and a heart valve testing chamber. In order to expose the valve to realistic pediatric flow conditions, six unique pump operating conditions were tested that involved pre-determined heart rate and stroke volume combinations. In addition, a modified aortic root model was used to hold the mechanical heart valve in place within the loop and to provide more realistic aortic root geometry. This heart valve chamber was made from a transparent acrylic material, allowing for fluid flow visualization. A traditional Particle Image Velocimetry (PIV) experimental set up was used in order to illuminate the particles seeded within the fluid path, and thus allowing for the capture of sequential images using a high speed camera. The data collected throughout this study consisted of flow rate measurements using an ultrasonic flow meter, and the sequential PIV images obtained from the camera in order to analyze general flow characteristics across the pediatric valve. Such information regarding the flow profile across the valve allowed for conclusions to be made regarding the valve performance, such as average flow velocities and regions of regurgitant flow. By gaining a better understanding of the fluid dynamic profile across a pediatric sized heart valve, this may aid in the eventual approval of pediatric sized mechanical heart valves for future clinical use.

1 INTRODUCTION

1.1 Motivation and Significance

Valvular heart disease is a life-threating condition that affects millions of people worldwide, leading to approximately 250,000 heart valve replacements each year [1]. Although more prevalent in the adult population, congenital heart valve disease is one of the most common abnormalities found in children. Valvular heart defects in children can be seen on both the systemic and pulmonary side of the heart, with the most common valve defects being mitral stenosis, aortic stenosis, and valvular regurgitation [2]. Such structural valve abnormalities adversely affect the blood flow across the diseased valve, and therefore affect blood flow throughout the rest of the body. Congenital heart valve defects occurs in approximately 1 in 150 children, being one of the most common abnormalities present at birth [5]. As a child's cardiac anatomy is significantly smaller than that of an adult patient, pediatric valve replacement presents unique surgical challenges for physicians and is often characterized as a high-risk procedure. Commercially available heart valve prostheses are often too large for a child's anatomy, creating a variety of additional surgical complications. Typically an enlargement procedure is performed in order to accommodate the prosthetic heart valve, which creates additional risks of injury to adjacent cardiovascular structures [2].

Currently, there are no FDA approved mechanical heart valves suitable for the pediatric population, and smaller sized commercially available valves are limited. The pediatric population has been excluded from replacement heart valve clinical trials due to a limited patient pool, complex health histories in children, limited valve sizes, and the need for additional valve replacements throughout the lifetime of a study due to the rapid growth of a pediatric population

[2]. As inappropriately sized pediatric valve replacements create additional complications, the need for appropriately designed and approved pediatric sized valves remains a pressing challenge in the medical device industry. In order to expedite the approval of appropriately sized pediatric heart valves for future clinical use, knowledge of the fluid dynamics across the valve must first be explored in order to assess the hemodynamic performance of pediatric sized heart valves.

1.2 Heart Valve Function and Anatomy

The human heart functionally serves as a pump, sending oxygenated blood and nutrients to various areas of the body. The human heart consists of four chambers and four major valves. The four chambers consist of the right atrium, right ventricle, left atrium, and left ventricle. The two atrioventricular (AV) valves lie between the atria and the ventricles, consisting of both the mitral valve and tricuspid valve. The mitral valve lies between left atrium and left ventricle, whereas the tricuspid valve lies between the right atrium and right ventricle. The two semilunar (SL) valves, the aortic and pulmonary valve, lie between the ventricles and the exit arteries allowing blood to exit the heart. The primary function of the four heart valves is to ensure unidirectional flow throughout the heart, playing a vital role in the overall performance of the heart and thus blood supply throughout the body. A diagram of the four chambers and four valves can be visually depicted in Figure 1.1.

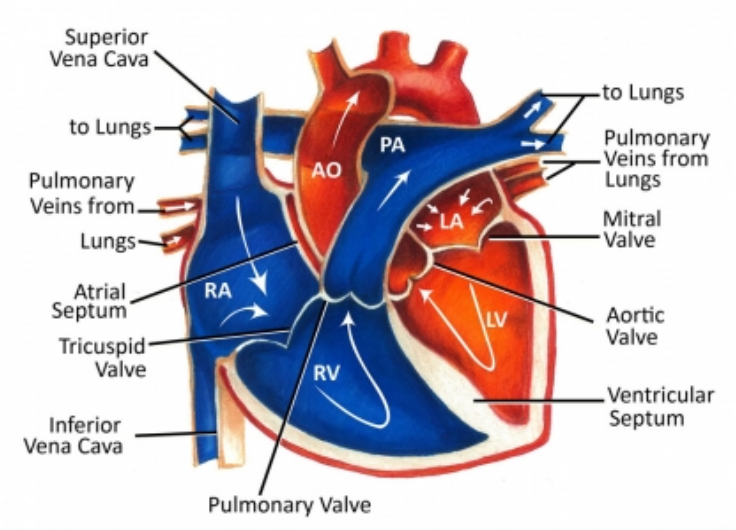

Figure 1.1: Heart Chambers and Valves

1.2.1 Right Heart Anatomy

The right side of the heart is responsible for transporting CO_2 rich blood to the lungs. Blood enters the right atrium via the superior and inferior vena cava, and then enters the right ventricle via the tricuspid valve. The tricuspid valve contains three leaflets that are attached to papillary muscles by chordae tendineae located in the right ventricle. The primary function of the chordae tendineae is to provide stability for the tricuspid valve, using tension to prevent prolapse of the leaflets into the atrium. During atrial systole, chordae tendineae are relaxed to allow the movement of blood from the atria to the ventricle. During this phase, pressure is higher in the atria than the ventricle, allowing blood to flow down the pressure gradient. During ventricular systole, the tricuspid valve closes due to increased pressure in the chambers. The chordae tendineae provide tension to the tricuspid valve during this phase in order to provide a tight closed seal, preventing back flow of blood into the atrium.

During the systolic phase of the cardiac cycle, the right ventricle pumps blood through the pulmonary arteries to the lungs via the pulmonary valve. Once the blood has entered the

lungs, the blood undergoes a CO_2-O_2 gas exchange via diffusion mechanisms. The pulmonary valve also contains three leaflets, and is opened due to the increased pressure in the right ventricle during systole. The pulmonary valve then closes at the end of systole, when right ventricular pressure begins to drop.

1.2.2 Left Heart Anatomy

The left side of the heart is the primary pumping mechanism responsible for systemic circulation, allowing oxygenated blood to reach various tissues, muscles, and organs of the body. Oxygenated blood enters the left atrium from the pulmonary veins, and is subsequently pumped into the left ventricle through the mitral (biscupsid) valve [4]. In contrast to the tricuspid and pulmonary valves of the right side of the heart, the mitral valve only contains two leaflets. The orifice is surrounded by a ring of fibrous tissue, the annulus. Similarly to the tricuspid valve, the mitral valve leaflets are connected to papillary muscles residing in the left ventricle. The mitral valve opens due to increased pressure in the left atrium as it fills with blood. An initial surge of blood enters the left ventricle and accounts for 70-80% of the total filling volume, whereas the remaining 20% of blood volume results from atrial contraction. As the pressure in the left ventricle increases due to filling, the mitral valve closes in order to prevent back flow. Due to the left side of the heart experiencing a larger pressure gradient than the right side of the heart, and therefore producing higher blood velocities, the mitral valve is typically the most common valve to be replaced in adults [4].

Once pressure in the left ventricle surpasses pressure in the aorta, the aortic valve opens and allows for blood to exit the ventricle and flow into the aorta. Once ventricular systole is complete, pressure in the left ventricle quickly drops and allows for the closure of the aorta valve. The aortic valve contains three leaflets; the right coronary, left coronary, and

noncornonary leaflets. In contrast to the mitral and tricuspid valves, the aortic valve is directly attached the vessel wall at the basal attachment and not supported by papillary muscle attachments. Attachment of the three leaflets forms the annular ring, separating the aorta from the left ventricle [1]. Superior to the annular ring is the aortic sinus, a structure containing three bulges at the root of the aorta. During closure of the aortic valve, the unbound edges of the three leaflets join together to form a seamless junction in order to prevent backflow, known as coaptation.

To compensate for the heavier and nutrient-rich blood the left ventricle must push throughout entire systemic circulation, the left ventricle muscle wall is much thicker in comparison to the right ventricle. The mitral valve must withstand pressures up to 150 mmHg, whereas the pulmonary and tricuspid valves must withstand pressures around 30 mmHg [1]. By having a more dense muscle wall surrounding the left ventricle allows for the generation of more physical pumping force from the left ventricle. Due to the difference in workload between the right and left side of the heart, the left side of the heart experiences much higher forces and more strenuous conditions. As a result, left sided heart valves are often more at risk for failure as they undergo larger amounts of stress. Figure 1.2 displays left ventricular pressure, volume, aortic pressure, and atrial pressure during phases of the cardiac cycle.

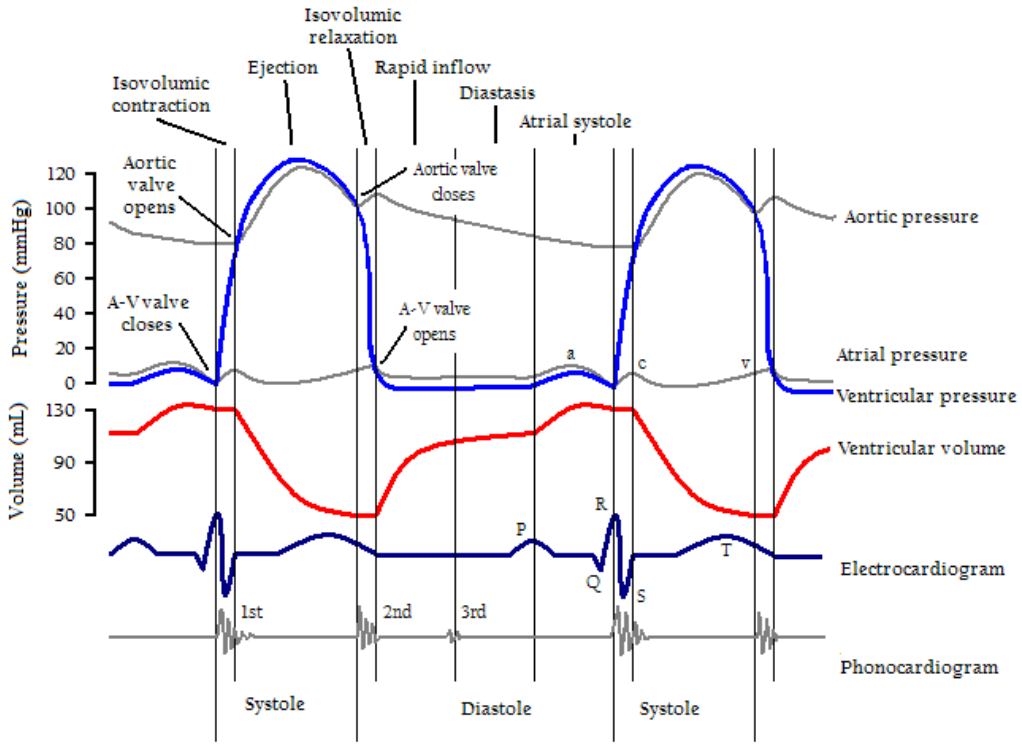

Figure 1.2: Pressures and Volumes of Cardiac Cycle

1.3 Congenital Heart Valve Diseases

The most common heart valve defects in the pediatric population include aortic stenosis, mitral stenosis, pulmonary stenosis, and valvular regurgitation. As mentioned previously, congenital heart valve defects remains one of the most common abnormalities present in children at birth. Typically, such defects are often associated with additional structural abnormalities that may require additional surgical intervention [2]. The most common heart valve defect found in the pediatric population is valvular regurgitation, which can affect the mitral, aortic, and pulmonary valves. Valvular regurgitation is often caused by catheter-based or surgical intervention aimed to treat severe valvular stenosis [1, 2]. Stenosis, or the narrowing of the native valve, is also a common valve defect often seen in the pediatric population. Based on the definitions provided in the June 2003 Pediatric Expertise for Advisory Panel [2], the pediatric

population consists of newborns (birth to 1 month), infants (1 moto 1 yr), toddlers (1-4 yr), children (5-12 yr), and adolescents (13-21 yr).

1.3.1 Aortic, Mitral, and Pulmonary Stenosis

Aortic stenosis involves the narrowing of the native aortic valve. This particular valve defect affects approximately 6 of every 1000 babies born [12]. Aortic stenosis can occur as an isolated defect, or in association with the aortic valve leaflets, ventricular septal defect, mitral valve abnormalities, and less commonly with atrial septal defect [12]. Due to this narrowing of the valve, the resistance of blood flow through the aorta is increased, generating a larger pressure drop across the valve. Due to this increased resistance of blood flow, a lesser amount of blood is able to pass through the aortic valve and to the rest of the body. Aortic stenosis in children can range from mild, moderate to severe. For children diagnosed with aortic stenosis after birth, appropriate treatment is determined by a variety of factors such as location of the narrowing, severity, associated cardiac problems, age, and size [12]. Aortic stenosis in children can be treated surgically or by balloon dilation, which will be further detailed in the following section.

Congenital mitral valve stenosis involves the narrowing and thickening of the mitral valve, and is a very rare condition occurring in less than 4 out of 1000 infants with congenital heart disease [13]. Mitral stenosis can occur at the supravalvular, valvular, or subvalvular levels. Common associated cardiac abnormalities associated with mitral stenosis are aortic valve stenosis and subvalvular aortic stenosis. Mitral stenosis obstructs blood from entering into the left ventricle, causing left atrial pressure to rise in proportion to the severity of the narrowing. As a result, this also restricts pulmonary venous return into the left atrium, increasing pressure in the right side of the heart. Children diagnosed with severe forms of mitral stenosis are likely to require surgical catheterization or valve surgery.

Congenital pulmonary stenosis involves the narrowing and thickening of the pulmonary valve, and accounts for approximately 10% of heart defects diagnosed during childhood [12]. Pulmonary stenosis can occur by itself or is conjunction with a variety of congenital heart defects such as atrial septal defect or Tetralogy of Fallot. Due to the thickening of the pulmonary valve, resistance to blood flow from the right ventricle to the pulmonary artery is increased. The severity of narrowing is measured by the pressure difference across the affected area. The higher the pressure difference indicates a higher degree of narrowing and the harder the right side of the heart must work in order to deliver blood to the lungs. Mild pulmonary stenosis is when the pressure difference is less than 30-40 mmHg, moderate pulmonary stenosis is when the pressure is 40 to 60 mmHg, and severe pulmonary stenosis is when the pressure is greater than 60-70 mmHg [12]. Critical pulmonary stenosis is a term used in infants born with very severe narrowing (greater than 90 mmHg) and requires treatment soon after birth.

1.3.2 Mitral Valve Prolapse

Although very rare during childhood, mitral valve prolapse (MVP) is diagnosed when there is a backward bowing of the mitral valve leaflets into the left atrium as the ventricle contracts. The leaflets are commonly thicker than normal functioning leaflets, and sometimes mitral valve regurgitation is present. Mitral valve prolapse is often associated with connective tissue disorders, such as the Marfan syndrome [12]. This particular disease can be inherited from the child's parents. There are usually minimal or no major symptoms related to MVP, however if mitral valve leakage progresses over time surgical intervention or the use of antibiotics is sometimes needed.

1.3.3 Valvular Regurgitation

Valvular regurgitation or insufficiency occurs when a particular valve does not close completely and allows blood to flow back into a particular chamber of the heart. Valvular regurgitation is often reffered to as a “leaking” valve, allowing blood to flow in two directions during contraction of the valve. Valvular regurgitation in children is commonly acquired due to catheter-based or surgical intervention aimed at treating severe stenosis, and can occur in the aortic, mitral, and pulmonary valves [2]. Isolated valvular regurgitation is a rare occurrence, as it is commonly associated with valvular stenosis or a ventricular septal defect [14].Valvular regurgitation due to surgical intervention is one of the most common valve defects within the pediatric population.

When a valve becomes regurgitant, the heart must work increasingly harder in order to compensate for the back flow of blood. In the case of mitral valve insufficiency, where blood flows backwards from the left ventricle into the left atrium, the heart compensates by leading to an increase in left ventricle ejection volume. When the regurgitant fraction of blood reenters the left ventricle, the left ventricle experiences volume overload. The left ventricle compensates via the Frank-Starling mechanism, resulting in an increased left ventricular stroke volume. Although left ventricular stroke volume increases, total forward stroke volume typically decreases and leads to lower cardiac output. These may lead to numerous complications including pulmonary congestion, hypotension, and heart failure; depending on the severity and volume of the regurgitant blood flow. Mitral valve insufficiency can be developed in three clinically significant stages; acute, chronic compensated and chronic decompensated [29]. Figure 1.3 depicts acute mitral regurgitation, and what immediately occurs with left heart pressure and volume, the stage

in which the rergurgitant flow causes a sudden volume overload of the left atrium and left ventricle.

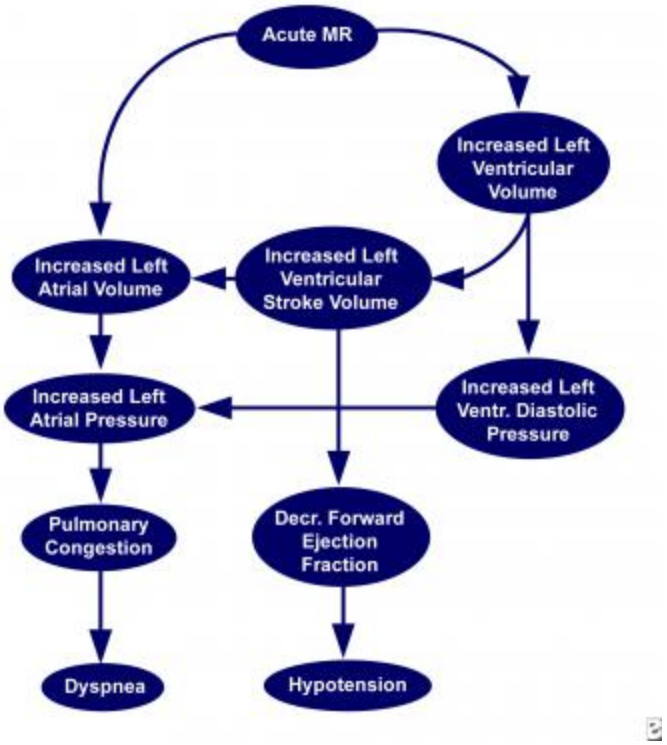

Figure 1.3: Acute Mitral Regurgitation [29]

1.4 Treatment of Congenital Heart Valve Disease

Depending on the severity of the heart valve defect, congenital heart valve disease can be treated using either catheter-based or surgical techniques. In some cases, both catheter based and surgical techniques are used for an individual patient with severe valve defects. Treatment of congenital heart valve disease using a catheter-based approach is desirable as it is easier on the child than open-heart surgery. However, sometimes surgery is required for particular defects that cannot be completely treated with catheter-based techniques. Figure 1.4 displays the distribution of valvular surgical procedures performed at the Children's Hospital in Boston, MA over a 5-

year period, separating each procedure in regards to the valve treated and if the treatment involved repair or replacement [2].

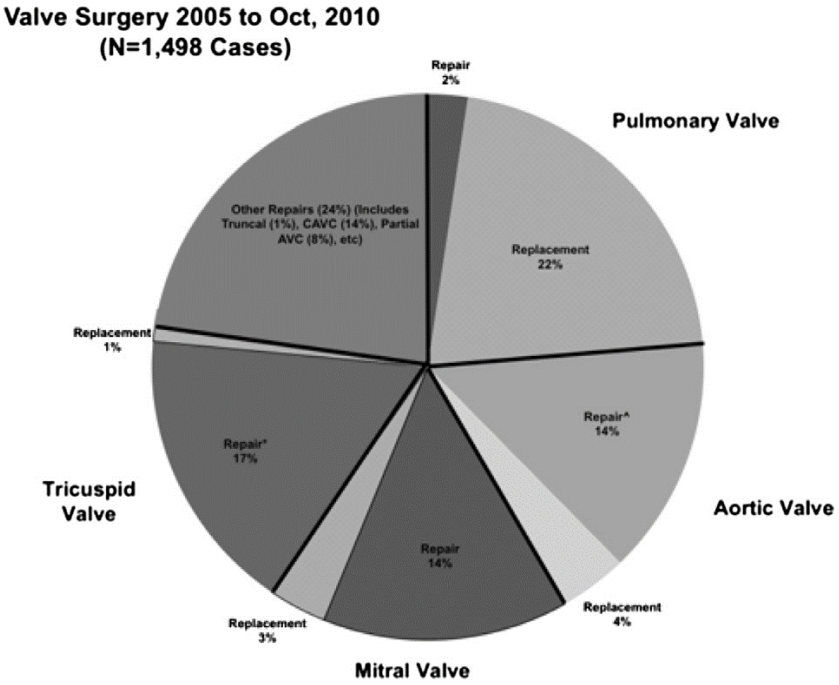

Figure 1.4: Distribution of Pediatric Valve Surgical Procedures [2]

1.4.1 Catheter-Based Techniques

Balloon Vavuloplasty is a common catheter procedure used to treat congenital valvular stenosis, in order to restore the valve's opening and closing abilities. During this procedure, a catheter with a balloon at the tip is threaded through a blood vessel in order to reach the diseased valve. The balloon is then inflated in order to facilitate the opening of the valve. After the valve has successfully been dilated, the balloon is deflated and both the balloon and the catheter tube are removed from the patient [6]. This method is currently the most commonly used method to treat congenital heart valve stenosis, as it is less invasive than surgical intervention. However, this technique carries the risk that the treated valve will later become regurgitant and require additional surgical intervention [2]. As a result, this procedure is viewed as a sufficient mid-term

solution, however should not be considered a life-long solution to heart valve abnormalities in children.

1.4.2 Surgical Valvotomy

An additional treatment option for children with severe valvular stenosis is direct incision of the fused leaflets of the valve during open-heart surgery [12]. During this procedure, a midline sternotomy incision is made down the middle of the chest and a heart-lung machine is used to support the patient while the valve is being repaired. This procedure is commonly performed when there is severe narrowing of surrounding structures in addition to the valve itself, often present above or below the valve. In such cases, a patch may need to be used to enlarge narrowed regions in addition to valve repair [12]. Mild residual narrowing and minimal valve leakage may occur, but oftentimes does not result in long-term problems. However, this approach is significantly more invasive than catheter techniques, which may lead to additional surgical challenges when operating on small children.

1.4.3 Ross Procedure

In the case of very young children and infants, balloon valvuloplasty and valve replacement prove to be extremely difficult for a variety of reasons [8]. As a result, the Ross Procedure is sometimes the recommended procedure for small infants. This procedure involves replacing the aortic valve with the patient's own pulmonary valve, and using a pulmonary allograft to replace the removed pulmonary valve [7]. This procedure is commonly used to treat aortic stenosis in infants and children. The advantages of using this procedure include growth potential, optimal hemodynamic performance, no need for anticoagulation medication, and less risk for hemolysis. However, some of the major concerns surrounding this procedure is the

potential dilation of the autograft, need for reoperation, and replacement of right ventricular outflow tract conduits [7]. In addition, this procedure aims to treat a single valve defect with a two-valve procedure, providing additional surgical demands and risks. Figure 1.5 visually depicts the Ross Procedure.

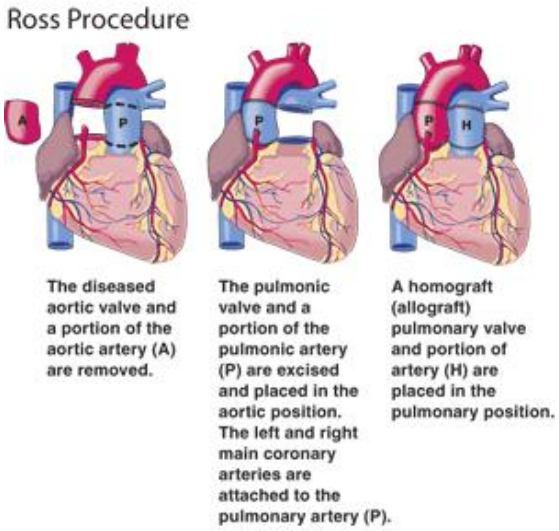

Figure 1.5: Ross Procedure

1.4.4 Valve Replacement

In the case where a diseased heart valve cannot effectively be treated with catheter-based or surgical techniques, the faulty valve may need to be replaced with either a mechanical or bioprosthetic heart valve. This often occurs when the diseased valve is too narrow or too leaky to surgically repair. Valve replacement in children is often viewed as a last resort, as both mechanical and bioprosthetic heart valves bring with them specific risks. Although mechanical heart valves prove very durable, thrombosis and the need for additional replacement as the child becomes older presents several disadvantages. Bioprosthetic heart valves offer the advantage of

superior hemodynamic performance, however the risk of calcification may also lead to the need for additional replacement. One of the major drawbacks to both mechanical and bioprosthetic valve replacement in children is the limited range of valve sizes available for the pediatric population.

1.4.4.1 Mechanical Heart Valves

Mechanical heart valves consist of three main elements; an occluder, the housing, and a sewing ring for proper implantation. There are three major mechanical heart valve classifications: caged-ball, tilting disc, and bileaflet valves. Mechanical heart valves come in a variety of sizes, however are mostly studied and utilized within the adult population. There are some smaller valve sizes available (17-19mm), however these sizes are not suitable for infants and very small children [9]. Although mechanical heart valves have experienced wide usage in adult patients, there still remains a limited number of pediatric-sized valves and there is currently no FDA-approved pediatric sized mechanical valve [1].

As there are limited available pediatric mechanical heart valve sizes, the available prosthesis chosen by the physician is often too large for the child's anatomy. This may result in delay in referral for surgery, as well as additional surgical techniques in order to enlarge the site of implantation to accommodate the prosthesis [1, 2]. Such enlargement procedures include the Nicks procedure, the Manougian procedure, and the Konno procedure, all of which involve annular enlargement [9]. Specifically, these procedures involve enlarging the left ventricular outflow tract and the valve ring by preforming an incision into the outflow tract of the right ventricle and the septum or wall between the right and left ventricles [12]. In addition, mechanical heart valves in children (and adults) require life-long anticoagulation medication to prevent thrombosis with its inherent risk of bleeding.

1.4.4.1.1 Caged-Ball Valves

The first successful mechanical heart valve implanted in a patient was developed by Hufnagel in 1952, consisting of a caged ball design [15]. This design gave way to the development of the Starr-Edwards aortic and mitral ball valves in the 1960s, with this design still currently being used clinically in the adult population. The housing of this caged valve is made from Stellite (a metal alloy of cobalt, chromium, molybdenum, and nickel), and the ball is made from Silastic Rubber® (silicone rubber) [15]. The Starr-Edwards caged ball valve demonstrates good reliability but poor hemodynamic performance. The flow goes through the annulus and around the silicone rubber ball, forming a circumferential jet that separates from the ball [1]. The caged ball valve produces a large pressure drop due to the high profile of the ball, in comparison to that of both tilting disc and bifleaflet valves. Due to caged-ball valves having a relatively large profile, they are not typically used for mechanical heart valve replacement within the pediatric population.

1.4.4.1.2 Tilting Disc Valves

Following the development of the caged-ball valve, the single leaflet tilting disc valve was developed in 1969 by Bjork-Shiley. This valve consists of a single pyrolytic carbon disk that is stabilized by inflow and outflow metal alloy struts. This design demonstrated improved hemodynamics, as the single disc serves as a partial occluder to flow rather than central occlusion produced by the caged-ball valve. Currently, the most common tilting disc valve used in the adult population is the Medtronic-Hall tilting disc valve, which consists of a titanium frame and a pyrolytic carbon disc. During systole, two high velocity jets flow from both the major and minor orifice outflow regions [1]. The flow on each side of the strut is almost symmetric, demonstrating very similar structural organization and velocities. Tilting disc valve

designs often demonstrate lower regurgitant volumes than bileaflet designs, with smaller valves demonstrating lower regurgitant volumes. Leakage flow through the gap between the disc and the housing of the valve often produces jets, which prove useful in the potential washing of the gap region [1]. This washing effect minimizes the formation of thrombosis around the gap region of the tilting disc valve. Although most tilting disc valves are designed for the adult population, there are some smaller sizes available (17-19mm) that are sometimes used for younger patients.

1.4.4.1.3 Bileaflet Valves

In the late 1970s, bileaflet valves composed of pure pyrolytic carbon-based leaflets were introduced. The bileaflet valve designs currently being used today consist of the St. Jude Medical bileaflet valve, Carbomedics bileaflet valve, and the On-X valve. These designs differ in the design of the hinge mechanism and the opening and closing angle, however both consist of pyrolytic carbon housing and leaflets, and a Dacron sewing ring. The bileaflet valve has become the gold standard of mechanical heart valves for most surgeons due to its favorable hemodynamic performance and anti-thrombogenic characteristics [15]. The St. Jude bileaflet valve, the more popular of the two designs, consists of a washout effect as the blood flows across the space between the leaflets, reducing the possibility of blood clot formation in those areas of the valve. The forward flow of a bileaflet valve is characterized by a triple-jet pattern, with two lateral orifices and one central orifice. After traveling approximately 20-30 mm downstream (for a 27 mm sized valve) the three jets merge into a central flow region [1]. Figure 1.6 displays the three major classes of MHVs currently being used.

Figure 1.6: (From Left to Right) Starr-Edwards Caged-Ball Valve, Medtronic Tilting Disc Valve, St. Jude Bileaflet Valve

1.4.4.2 Bioprosthetic Heart Valves

Bioprosthetic valves are replacement valves derived from either animal or human heart tissue, and have also been used as an option for valve replacement in children. Bioprosthetic valves come in a variety of sizes and types, however sizes under 19 mm are unavailable. As a result, bioprosthetic valves are not suitable for small children and infants even if enlargement techniques are used [9]. As bioprosthetic valves more closely match the anatomy of a native heart valve than a mechanical heart valve, their hemodynamic performance is often superior to that of mechanical heart valves. As a result, thrombosis is less of an issue with bioprosthetic valves and the patient is not required to be on anticoagulants. However, calcification of available bioprosthetic valves remains a major issue and may lead to the need for reoperation. The occurrence of calcification in porcine bioprostheses and autologous pericardia is higher in children than in adults, which accounts for the poor durability such valves present in regards to pediatric applications [10]. As with mechanical heart valves, there is a limited pool of available bioprosthetic heart valves suitable for the pediatric population.

1.5 *In-Vitro* Fluid Mechanics of Mechanical Heart Valves

Many of the complications that arise with mechanical heart valves are often associated with the fluid mechanics of particular valve designs. Therefore, there is a need to evaluate valve performance through *in-vitro* studies that aim to recreate the physiological conditions valves undergo within the body. From an engineering perspective, the ideal heart valve should 1) produce minimal pressure drops across the valve, 2) produce relatively small regurgitation volumes, 3) minimize turbulence, 4) minimize regions of high shear stresses, and 5) not create stagnation of flow separation regions in the flow fields in its immediate vicinity [1]. All such factors can be investigated in in-vitro experimental set ups in order to better assess a particular mechanical heart valves' viability *in-vivo.*

A pressure drop is a measure of flow potential energy losses that occur when viscous blood flows through a heart valve, and is an indication of heart valve efficiency [1]. A mechanical heart valve design should not significantly restrict the flow of blood, thus should produce a minimal pressure drop across the valve. The effective orifice area (EOA) and performance index (PI) are indices of how successfully a valve uses its primary or internal stent orifice area. The EOA is defined as [1]:

$$EOA = \frac{Q_{rms}}{51.6\sqrt{\Delta p}}$$

where Q_{rms} represents the root mean square systolic/diastolic flow rate and Δp represents the mean systolic/diastolic pressure drop. A larger value of a valve's EOA indicates a smaller pressure drop, and therefore a smaller energy loss. The performance index (PI) is also a measurement of a valve's resistance to forward flow, and is represented as the ratio of the EOA to the valve's sewing ring area [1]. Thus, the PI normalizes EOA by the valves size.

Regurgitation in mechanical heart valves occurs from reverse flow during valve closure and leakage, and is typically measured by percentage of stroke volume. Regurgitant volume is represented as the sum of closing volume and leakage volume, with closing volume being the total volume of retrograde flow during valve closure and leakage volume represents any fluid accumulation after valve closure. The amount of regurgitant volume depends on both valve type and size, increasing as valve diameter increases [1]. It is common for mechanical heart valves to display larger amounts of regurgitation as opposed to bioprosthetic valves. Although major valvular regurgitation may cause complications, minor regurgitation is sometimes desirable in certain valve designs in order to produce washout effects.

Other important fluid mechanics parameters that determine a valves performance are flow velocities and regions of shear stress in both immediate vicinities of the valve as well as within the valve. Flow field characteristics and shear stress regions vary depending on valve type and size, presenting the need to investigate fluid mechanics behavior in in-vitro studies prior to clinical use. Both flow fields and areas of high shear stress are often attributed to valve complications, such as thrombosis and hemolysis. Regions of flow stagnation and/or separation have been connected to thrombus formation, tissue overgrowth, and calcification [1]. Regions of high shear stress may lead to damage to red blood cells such as hemolysis, as well as platelet activation. Therefore, flow velocities and regions of shear stress are two major parameters to be studied when analyzing the fluid dynamics of a mechanical heart valve.

Another fluid characteristic of mechanical heart valves is the occurrence of cavitation, which is defined as the formation of vaporous or gaseous bubbles caused by a local pressure drop and their following collapse when pressure is recovered [34]. Some of the factors associated with MHV cavitation include valve closing velocity, ventricular loading rate, squeeze flow, valve

mounting, and occluder material properties. When the bubbles collapse after pressure has been recovered, high velocity fluid jets and pressure waves are produced which are capable of causing blood and valve material damage. Valve material erosion and pitting damage due to cavitation has been reported in many *in-vitro* studies, as well as blood damage such as hemolysis has been reported in *in-vitro* and *in-vivo* studies [34]. Therefore, minimizing the occurrence of cavitation remains a top priority in the development of mechanical heart valves.

1.5.1 Clinical Complications Related to Fluid Mechanics of MHVs

One of the major clinical complications associated with mechanical heart valve fluid behavior is the initiation of thrombosis around various valve components, which can be attributed to both the hemodynamic profile of the valve as well as the valve material. Since this study is focused on fluid dynamics, this review will omit the relationship between clinical complications and valve material. The initiation of a thrombotic event involves a complex set of protease reactions involving roughly thirty unique coagulation proteins [33]. The final outcome of these reactions is the conversion of fibrinogen, a soluble protein, into insoluble strands of fibrin through an active enzyme thrombin [33]. In conjunction with activated platelets, the fibrin strands form a stable blood clot. The complex geometrical designs and dynamic opening and closing behavior of MHVs can result in non-physiological flow conditions that may bring arise to turbulence, vortices, stagnation, and flow separation. Such flow phenomena produce high local shear stresses that can lead to the activation of platelets and some coagulation proteins, resulting in thrombus formation in localized regions of the valve. Some research has shown that the Von Williebrand Factor (VMF), a large blood glycoprotein, plays an important role in the shear-induced platelet activation [33]. Specifically, several studies have shown that the shear-

mediated conformational changes of VMF facilitates its binding to platelets, eventually leading to thrombus formation in local regions of high shear stress within the valve [33].

In addition to thrombosis of MHVs, hemolysis is also a major clinical complication associated with the fluid mechanics behavior of MHVs. As early as 1970, Harker and Slicther [22] showed that patients with mechanical heart valves exhibited a shortened platelet half-life caused by platelet activation and destruction. Mechanical trauma caused by the valve structure itself as well as high shear stresses caused by flow turbulence are both viable causes for such destruction of red blood cells and platelets. Due to the nature of flow across a MHV, the flow can be characterized as very complex and highly unsteady, and at times turbulent. Such flow behaviors brings arise to a variety of clinical complications, such as thrombosis and hemolysis, therefore it is important that sophisticated experimental and computational techniques are used in order to test the viability of a particular mechanical heart valve design.

1.5.2 History of *In-Vitro* Evaluation of Mechanical Heart Valves

Dating back to the 1970s, investigations of the fluid mechanics of MHVs have been conducted in order to better assess the performance of a wide variety of MHVs. Such studies have used varying experimental setups and have tested both FDA-approved and unapproved valve designs. Some of the major topics focused on in such studies include regurgitant flow behavior, vortex and microbubble formation, valve closure, cavitation potential, as well as investigating the flow region near the hinges of certain valves. Such research has provided useful information regarding MHV performance and design and has led to the development of many MHV designs. This section of this paper will review the history of experimental studies of prosthetic heart valve flow dynamics.

In 1975, Brown *et al* [16] conducted one of the first experiments that investigated the relationship between thrombus formation and shear stress, one of the major complications associated with MHVs of all types. From this study, they found that platelets exposed to shear stresses over 50 dyne cm^{-2} release a larger amount of ADP and had a tendency to aggregate faster than platelets exposed to lower values of shear stress [16]. This finding showed that shear stress could induce platelet aggregation, which may led to the damage of surrounding red blood cells. Therefore, identifying regions of high shear stress within the flow pattern across a MHV has remained a major topic of interest when investigating fluid behavior of MHVs.

Laser Doppler Velocimetry (LDV) is an experimental technique involving the use of the Doppler shift in a laser beam in order to measure the velocity in transparent fluid flows, and has been used extensively in the investigation of MHV fluid dynamics. Using 1D LDV, Chandran *et al* [17] investigated flow fields distal to that of caged ball and tilting disc aortic valves. They concluded that both the velocity profiles and turbulent shear stresses downstream from the tilting disc valve were directly dependent on the opening behavior of the valve. Additionally, they concluded that the turbulent shear stresses downstream the caged ball valve were smaller in magnitude than that of the tilting disc valves. Using 2D LDV, Yoganathan *et al* [18] developed a detailed study of the pulsatile forward flow fields of both the St Jude Bileaflet valve and the Bjork-Shiley tilting disc valve. Their results indicated maximum shear stresses of 1200 dynes cm^{-2} for the bileaflet valve and 2000 dynes cm^{-2} for the tilting disc valve. Using 3D LDV, Fontaine *et al* [19] studied the flow fields of both Bjork-Shiley and St. Jude bileaflet valves, and produced results very similar to that of 2D LDV studies (values within 10-20%).

Another major topic that has been widely investigated through in-vitro studies of MHVs is the occurrence of retrograde flow across the valve. Although most MHVs are deliberately

designed to include some degree of retrograde flow in order to wash out certain areas of the valve, regurgitant flow has also been attributed localized regions of high shear stress and vortex formation. Yoganathan *et al* [18] found that the peak reverse velocity through a Medtronic-Hall tilting disc valve was 0.28 ms^{-1} with a peak shear stress of 680 dyne cm^{-2} under pulsatile aortic conditions. Meyer *et al* [20] showed that leakage flows are capable of producing turbulent jets with elevated Reynolds shear stresses even in bileaflet valves, with maximum regurgitant velocities ranging from 0.7 to 2.6 m/s and maximum shear stresses ranging from 450 to 3,600 dyne cm^{-2} after valve closure. Their results allowed them to predict regurgitant leakage flow regions with different MHV designs, identifying that the hinge region of bileaflet valves are the principle site of leakage whereas the gap between the disk and the support ring is the principal site of leakage for tilting disc valves [20]. Identifying the regions and magnitude of leakage for a particular MHV, can lead to the development of improved designs that may offer more favorable hemodynamic performance.

The investigation of valve closure dynamics and associated cavitation potential began in 1989, when clinical failures of Edward-Duromedics valves were reported [22]. These valves were noted with both pitting and erosion features, indications of mechanical cavitation damage. Cavitation is the process of both the growth and collapse of vaporous and gaseous bubbles in a liquid, and is often caused by a sudden pressure drop often attributed to valve occluder closure. When such bubbles collapse, micro-jets may form and cause localized erosion damage to occluder material as well as blood damage. There are many additional factors that influence MHV cavitation, including ventricular loading rate, squeeze flow, valve mounting, and occluder material properties [21, 22]. The evaluation of cavitation near MHVs has primarily been focused on visualization of bubble formation in transparent media, however recent studies have shown

more quantitative methods of evaluation. Lamson *et al* [21] presented a study in which MHV cavitation patterns were detected in real time. By using a real time detection process, they were able to develop a cavitation cycle that corresponds to a normal cardiac cycle. Such studies have led to the exploration of the both the causes and locations of MHV cavitation, which aids in the development and design of MHVs.

1.5.3 Mechanical Heart Valve Experimental Setups

In order to achieve reliable data concerning mechanical heart valves, an effective simulation of the native heart environment must first be achieved. In order to do so, a typical experimental set up consists of a mock circulatory loop to simulate appropriate flow conditions in addition to a valve holding chamber and image capture system. Depending on the intended goal of a particular experiment, both the design of the mock loop and valve chamber may vary. For instance, some studies may choose to focus on reproducing specific flow conditions whereas some studies may choose to focus on anatomical correctness. The following section will discuss some of the valve testing chambers and mock loops that have been used and their purpose in that particular study.

1.5.3.1 Mechanical Heart Valve Testing Chambers

As mentioned previously, MHV experimental set up is largely focused on the particular intent from the study. For instance, Browne *et al* [23] focused on investigating turbulent flow downstream of a St. Jude bileaflet valve using both laser Doppler velocimetry (LDV) and Particle Image Velocimetry (PIV), and comparing the two imaging modalities. Since this particular study focused more on the comparison of the two imaging techniques, compliance and peripheral resistance were neglected. Their main focus was effectively imaging downstream of

the valve, therefore their MHV testing chamber consisted of a clear, anatomically correct aortic root model. The aortic root model was made from a solid acrylic block, and incorporated a native sinus section. Figure 1.7 displays the aortic root model used in this study.

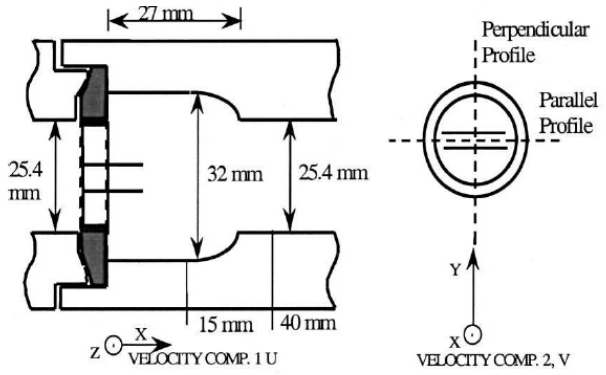

Figure 1.7: Aortic Root Model

Manning *et al* [24] sought to investigate the regurgitant flow field characteristics of a St. Jude bileaflet valve both in localized regions within the valve and in regions distal to the valve. This particular study utilized a "single shot" chamber system which consisted of a transparent two compartmental box in order to mount the valve in the mitral position. The larger component represented the left atrium and was open to the atmosphere, whereas the smaller component represented the ventricle and was sealed and connected to pneumatic pressure regulator system. This particular system simulated the reverse flow characteristics of the cardiac cycle with minimal forward flow through the valve, allowing better investigation of regurgitant characteristics. An anodized aluminum valve holder was placed between the two chambers in order to hold the valve in place throughout the duration of the study. Figure 1.8 visually depicts the "single shot" chamber system used in this particular study.

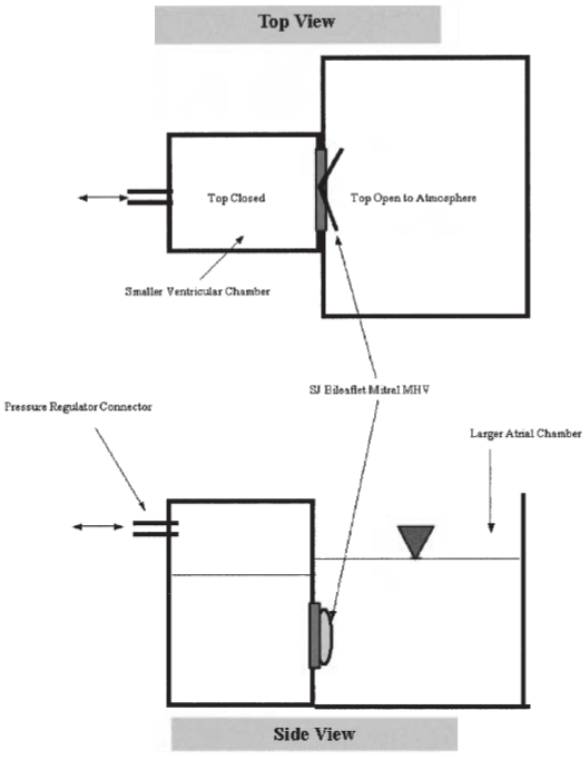

Figure 1.8: “Single Shot” Chamber System

Manning et al [25] later went on to investigate the near valve flow characteristics of a Bjork-Shiley tilting disc valve using a modified version of the “single shot” chamber system. The aim of this particular study was to better understand the local fluid mechanics that occur during MHV closure and rebound, including the influence of the regurgitant jet and its relationship to cavitation. Since this particular study focused on near-valve flow characteristics, a modified single shot chamber with more realistic near valve geometry was used. This modified chamber included a more confined expansion/contraction on either sides of the valve, representing the sinus area. Although this approach was not completely anatomically correct, it provided a more realistic restriction to flow found in the native left atrium and ventricle. This particular chamber only simulated the closing phase of the MHV, as that was the primary focus of this study. Figure 1.9 shows the set up for the modified single shot chamber.

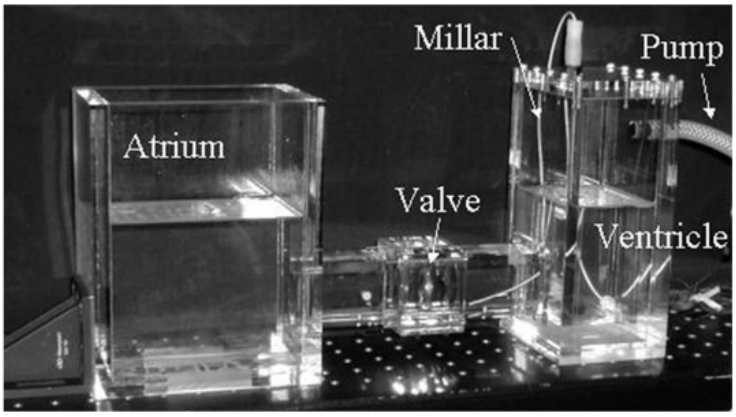

Figure 1.9: Modified "Single Shot" Chamber

1.5.3.2 Mock Circulatory Loops

Mock circulatory loops have been extensively used for the *in-vitro* testing of various cardiovascular devices, a critical process necessary prior to clinical trials of any medical device. Mock circulatory loops are designed to represent the human cardiovascular system to allow for the testing of artificial heart valves, ventricular assist devices (VADs), total artificial hearts, and other cardiovascular devices. More basic systems consist of a pre-load chamber to produce a constant flow and a resistance valve to alter the pressure drop [26]. Newer systems may involve pulsatile flow, adjustable compliance and resistance, and other cardiovascular components. The design and implementation of a mock circulatory loop is heavily dependent on the researcher's aim of their particular study.

Many of the earliest mock circulatory loop designs were pulse duplicators driven by steeping motors and linear actuators. Based on a larger design proposed by Davila, Trout, Sunner, and Glover in 1956, Bjork *et al* [27] introduced a pulse duplicator capable of controlling systolic-diastolic ratio, stroke volume, and cardiac output in order to test mitral and aortic prosthetic valves. The pulse duplicator consisted of two independent hydraulic systems; 1) a

pumping system consisting of a one-armed roller pump capable of regulating stroke volume and pulse rate and 2) a testing system capable of representing the left ventricle, aorta, peripheral resistance, and the left atrium. The results of this study showed the importance of simulating left ventricular, atrial, and aortic dynamics during the testing of prosthetic valves. Due to the success of this study, many future studies involving the testing of prosthetic valves employ very similar mock loop configurations. Figure 1.10 displays a schematic drawing of the pulse duplicator used in this study.

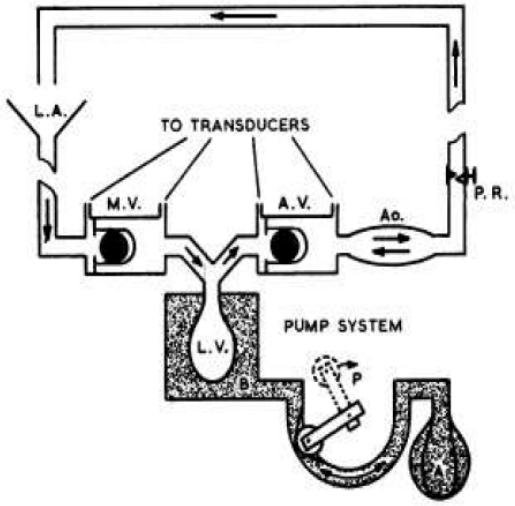

Figure 1.10: Pulse Duplicator. LA=left atrium, MV= mitral valve, LV = left ventricle, P = pump, AV = aortic valve, Ao = Aorta, PR = peripheral resistance, A = elastic container.

Overtime, other mock circulatory system designs were proposed that contained additional cardiovascular elements to provide a more realistic physiological environment to test cardiac devices. The Pennsylvania State University Mock Circulatory Loop System described by Rosenberg [28] added new components such as waveform generators, compliance chambers to stimulate arterial and venous compliance, systemic resistance elements, and a venous reservoir. This system was initially designed in 1971 for the testing of ventricular assist devices, however

has also been modified for the testing of mechanical heart valves. In addition, this system implemented pressure transducers and flow meters in order to better monitor and assess the fluid flow throughout the system. Figure 1.11 shows a diagram of the Penn State Mock Loop used for the testing of an Electric Ventricular Assist Device.

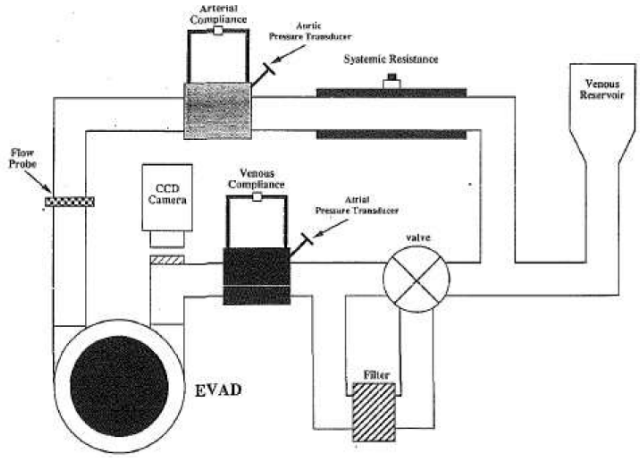

Figure 1.11: Penn State Mock Circulatory System

1.5.4 Pediatric Heart Valve *In-Vitro* Studies

Adult mechanical heart valves have been widely studied and analyzed, through both *in-vitro* and *in-vivo* studies. By using flow visualization techniques, such as Particle Image Velocimetry (PIV), the flow field characteristics of adult sized mechanical heart valves are well characterized. The characterization of flow dynamics is essential in determining the effectiveness of a mechanical heart valve, as flow features are often associated with heart valve complications such as thrombosis. In one pediatric study, it was concluded that thrombosis is the second most common problem of mechanical heart valves in children [11]. As pediatric sized heart valves are smaller in size, this may result in for increased blood damage due to different fluid dynamic conditions. Although there has been many *in-vitro* studies investigating the fluid dynamic conditions for adult valves, there remains minimal research regarding pediatric heart valve fluid

dynamics. Most studies focusing on pediatric valves have been limited to computational studies, therefore excluding *in-vitro* experimental studies.

1.5.4.1 Computational Studies

Although there has not been many *in-vitro* studies focusing on pediatric heart valves, there has been several attempts to analyze the fluid dynamics of pediatric valves using computer simulation. Specifically, Yoganathan *et al* [3] modeled a pediatric sized valve and flow conditions in order to assess blood damage in a bileaflet mechanical valve in 2014. In this particular study a model of an adult-sized 23 mm St. Jude Medical Regent valve is selected for the simulation, which is then scaled down in size to match the anatomy of both a 5-year old child and 6-month old infant. A previously validated lattice-Boltzmann method was used to stimulate pulsatile flow with thousands of suspended platelets for cases of adult, child, and infant flows [3]. The blood used in this particular study was modeled as an incompressible Newtonian fluid, and was modeled to have the same kinematic viscosity parameters as whole blood. The overall aim of this study was to gain a better understanding of the hemodynamics and blood damage performance of pediatric sized valves, which may help facilitate the approval of such valves to be used in children.

The results of this particular computational study exposed several differences in both the flow conditions and blood damage performance for the adult and child/infant simulations. Most notably, it was observed that adult flow showed more disorganized small-scale flow features at peak flow rates, whereas child and infant flow were characterized by larger, more coherent flow with weak recirculation [3]. With infant flow, no vortex wakes were observed however the flow was dominated by triple jet-like flow. In addition, infant flow showed much higher shear stresses than the adult case, which can be attributed to the coherent forward jets observed with the infant

flow. Platelet damage in the pediatric cases was higher than the adult case, indicating possible thrombus risks of pediatric valve flows. The highly damaged platelets overserved in the pediatric flow were often found downstream of the valve, as there was less recirculation in the pediatric flow cases. The differences between both the adult and pediatric cases from this study point out the need to further investigate flow properties of pediatric valves, and may push for the eventual approval of prosthetic valves for the pediatric population.

1.6 Research Aims

Congenital heart valve disease is one of the most common abnormalities in children, with common valve defects being aortic stenosis, mitral stenosis, and valvular regurgitation [1]. Although adult sized mechanical heart valve (MHV) replacements are widely studied and utilized, there are currently no FDA approved prosthetic heart valves available for the pediatric population. Much like adult sized mechanical heart valves, pediatric sized MHVs may experience potential clinical complications such as thrombosis, blood damage due to high shear stresses, and cavitation. Due to pediatric sized heart valves being much smaller than adult sized valves, different fluid dynamic conditions and associated complications are expected. In order to accelerate the approval of pediatric sized heart valves for clinical use it is important to first characterize and assess the fluid dynamics across the valve. By understanding the hemodynamic performance of the valve, connections can be made concerning potential valve complications such as thrombosis and cavitation. The overall goal of this study is to better characterize and assess the flow field characteristics of a pediatric sized mechanical heart valve using flow visualization techniques in a mock circulatory loop.

Although there have been many *in-vitro* flow field visualization studies for adult sized MHVs, there remains a very limited number of *in-vitro* and computational studies devoted

towards pediatric sized valves. Mock circulatory loops are often used to replicate the human circulatory system in order to assess the functionality and hemodynamic performance of a MHVs and other cardiac assist devices. By using flow visualization techniques, a better understanding of the fluid dynamics across a valve can be achieved and used to assist in future MHV design. This particular study intends to characterize the fluid dynamic performance of a pediatric sized MHV through the implementation of a valve testing chamber in a mock circulatory loop using appropriate physiological conditions, as there are a very limited number of studies that focus on pediatric sized valves. By gaining a better understanding of the fluid dynamic profile across a pediatric sized heart valve, this may aid in the eventual approval of pediatric sized mechanical heart valves for future clinical use.

Specific Aim #1: Modify existing mechanical heart valve chamber in order to accommodate a pediatric-sized mechanical heart valve.

Specific Aim #2: Implementation of valve holding chamber into mock circulatory loop under appropriate pediatric physiological conditions.

Specific Aim #3: Characterize flow field dynamics using flow visualization techniques in order to assess valve performance in regards to potential complications such as thrombosis and cavitation.

2 METHODS AND MATERIALS

2.1 Mock Circulatory Loop

In order to test and analyze the flow conditions across a mechanical heart valve, it is necessary to implement a mock circulatory loop system that is capable of simulating the human circulatory system. Therefore, a mock circulatory loop similar to that of previous cardiovascular research was used throughout this study. This particular mock loop consists of several key components; including a Harvard Apparatus Pulsatile Blood Pump to serve the functional role of the heart, a tank to serve as the venous reservoir, quick disconnect mechanisms, and a custom aortic root model to hold the valve. Each of these components play a critical role in replicating the human circulatory system, and can be adjusted accordingly to account for different physiological conditions, such as pediatric flow conditions. These components are connected with 1 ¼ inch outside diameter (OD) and ¾ inch inside diameter (ID) tubing that serves as the native vasculature. In order to measure certain circulatory parameters, several devices are installed throughout the system. With the expectation of the custom pediatric sized heart valve chamber modification, the design the implementation of the mock loop system were completed by Charles Taylor among other members of the Artificial Heart Laboratory at Virginia Commonwealth University [30]. Figure 2.1 displays an image of the entire mock loop used in this study with labeled components.

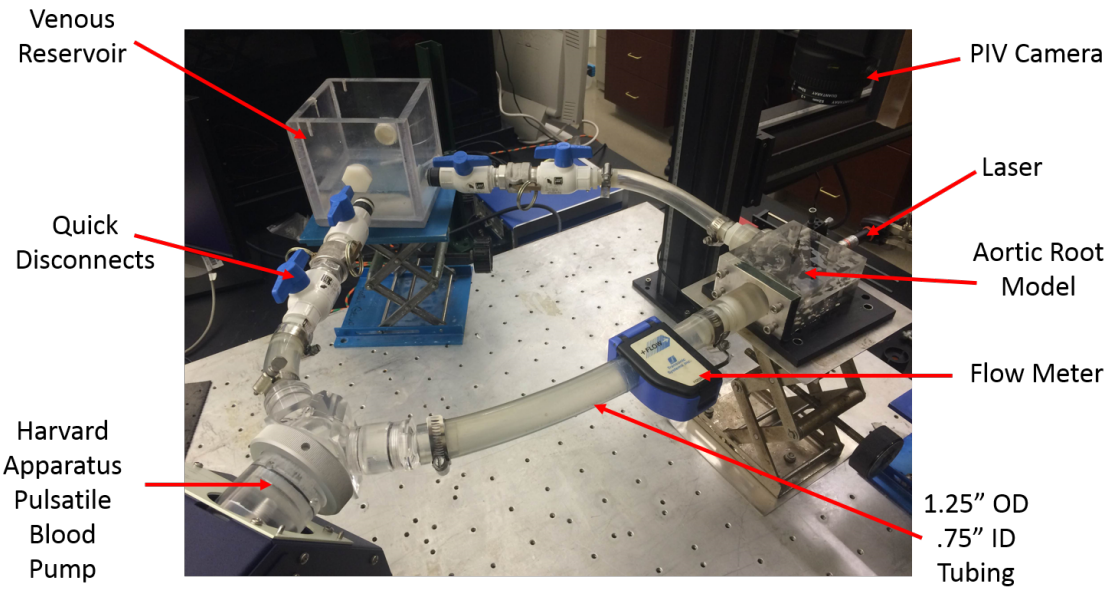

Figure 2.1: Mock Circulatory Loop

2.1.1 Venous Reservoir

The venous reservoir, which is represented as a 6" x 6" x 6" acrylic box, serves as the supply for the Harvard Apparatus pulsatile pump. The venous reservoir consists of a top open to the air, one inlet port and two outlet ports (Outlet Ports 1 and 2). The venous reservoir is open to the atmosphere to allow for the evaporation of trapped air within the system, allowing for the absence of bubbles throughout the tubing of the loop. The absence of air bubbles within the system allows for more accurate flow measurements and more reliable PIV images. Outlet Port 1 leads to the inlet of the pulsatile pump, whereas Outlet Port 2 may lead to the inlet of a ventricular assist device, when applicable. The tank is filled to a level just above the inlet port, to ensure the loop is completely filled and bubbles are absent from the system. By making adjustments to the fluid level in the tank and/or the height of the tank itself, the arterial pressure of the entire system can be varied accordingly. A magnetic stir bar is placed in the venous reservoir to ensure a homogenous mixture of the water/glycerin fluid. Figure 2.2 displays an

image of the venous reservoir used in this research, with fluid being filled to just above the outlet ports.

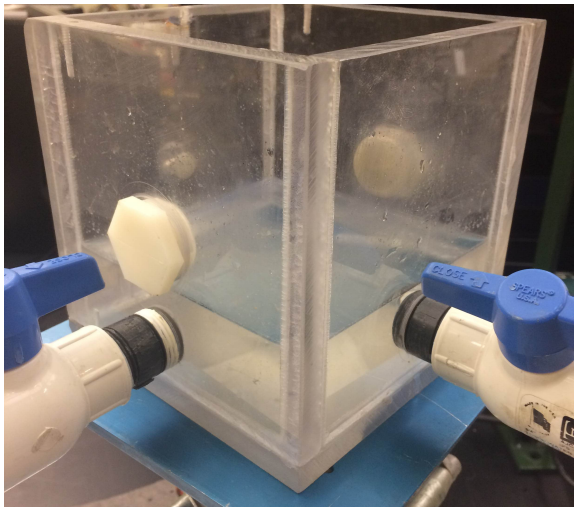

Figure 2.2: Venous Reservoir

2.1.2 Quick Disconnect Mechanisms

In between each outlet port of the venous reservoir and their respective connection, lie quick disconnect mechanisms. These mechanisms serve as flow facilitators throughout the entire mock loop, and allow for detachment of individual loop components without having to drain the entire system. Each mechanism consists of a metal on metal cam-and-groove hose coupling in conjugation with a low pressure PVC dual ball valve. By having such mechanisms in place, modifications to the loop configuration can be made with relative ease and minimal disturbance to the overall system. Figure 2.3 displays an image of the quick disconnect mechanism used in this research.

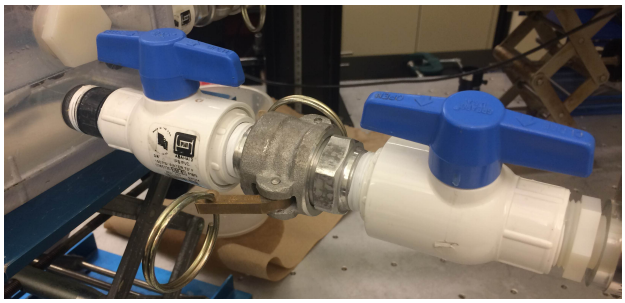

Figure 2.3: Quick Disconnect Mechanisms

2.1.3 Harvard Apparatus Pulsatile Pump

As mentioned previously, Outlet Port 1 of the venous reservoir tank serves as the inlet to a Harvard Apparatus Pulsatile Blood Pump Model 1423. This particular pump is a well-respected standard in hemodynamic research that aims to stimulate large animal cardiovascular systems. This pump intended to pump blood or blood analog with minimum damage to blood cells, which is ideal in hemodynamic research [32]. This particular pump consists of a mechanically activated piston that oscillates within a transparent cylindrical hub, and two caged ball valves located at the mitral (inlet) and aortic (outlet) positions, which can be seen in Figure 2.4. The valve cages and liquid pathway have been designed to provide a streamlined flow absent of sharp edges, minimizing hemolysis. All components of the liquid pathway of the pump can be disassembled and sterilized when necessary.

With this particular pump, both stroke volume (SV) and strokes per minute (Heart Rate, HR) can be dynamically adjusted while the pump is being utilized. The stroke volume is adjusted using a knob on the top of the pump, with the actual stroke volume read out coming from a calibrated plate on the side of the pump. The stroke volume can be adjusted from 15 mL to 100 mL. The strokes per minute, or “heart rate” can be adjusted using a dial on the end of pump opposite from the pump head. The strokes per minute can varied from 10 to 100 strokes per min

(BPM). In addition, this particular pump model is equipped with a control to adjust the ratio of systole to diastole (systolic duration or output phase ratio). This control is located adjacently to the rate control knob. The control is continuously variable from 25/75 to 50/50. In the 25/75 position, systole takes place 25% of the cardiac cycle while diastole takes place in 75%. By having control of stroke volume, heart rate, and systolic duration, this pump is capable of testing a wide range of physiological conditions.

In order to accommodate the testing of the pediatric valve farther downstream to represent the aortic positon, additional pump modifications performed in this research include the removal of the silicon ball in the outlet pump valve. The design of the pump allows for easy removal of such components, making it possible to remove the silicone ball-check valve.

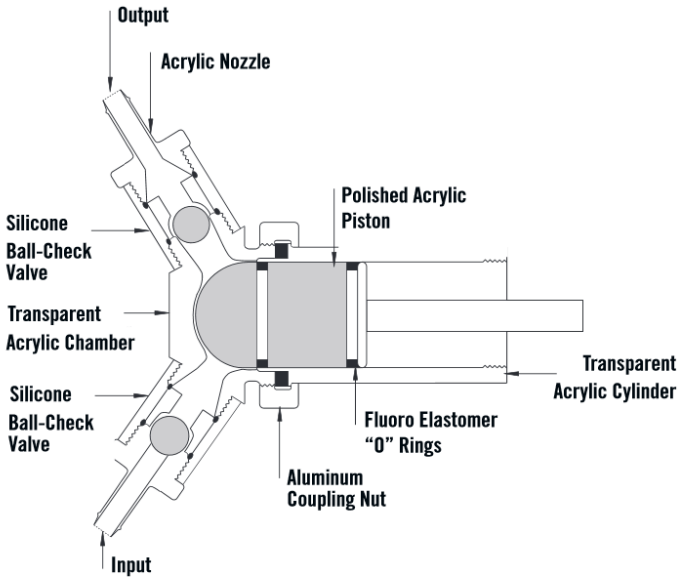

Figure 2.4: Harvard Apparatus Blood Pump [32]

2.1.4 Mechanical Heart Valve Testing Chamber

In order to visualize the flow across the heart valve, a modified version of an aortic root model previously developed by Charles Taylor [31] was used to mount the pediatric sized valve within the mock circulatory loop. The model is made entirely from transparent acrylic material, allowing for the visualization of flow patterns surrounding the valve. The geometry of this model was made by using female thorax cyro-slice datasets provided the Visible Human Project, in order to provide more realistic and accurate aortic root geometry [31]. This particular aortic root model was originally intended to house a 27 mm Bjork-Shiley Convexo-Concave tilting disc valve, therefore additional modifications were needed in order to accommodate the smaller sized heart valve. The valve selected for this study is a 17 mm Bjork-Shiley Convexo-Concave tilting disc valve, which is commonly used as a heart valve replacement in young children ranging in ages 5-12 years old [2]. Figure 2.5 displays a description of a Bjork-Shiley tilting disc valve and Figure 2.6 displays the aortic root model prior to any modifications.

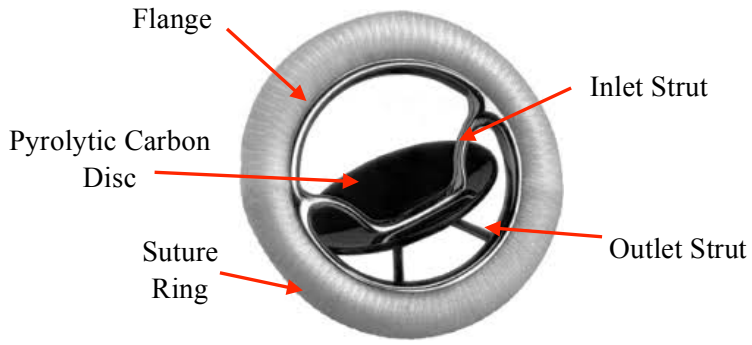

Figure 2.5: Bjork-Shiley Convexo Concave Tilting Disc Valve

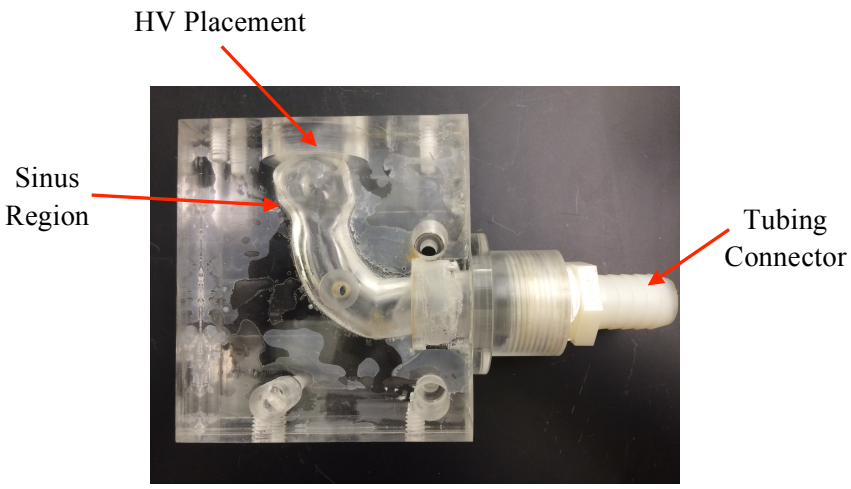

Figure 2.6: Transparent Acrylic Aortic Root Model

In order to accommodate the smaller heart valve in the opening where the 27mm valve was intended to be placed, an appropriately sized rubber O-ring was attached to the opening using silicone adhesive. The diameter of the O-ring is slightly larger than the diameter of the pediatric heart valve (17 mm), however small enough to ensure a tight seal around the valve. Silicone adhesive was chosen as the method to secure the O-ring to the original model as it is both transparent and water-resistant, which would allow fluid testing to be conducted without obstructing flow or the visualization of flow surrounding local regions of the valve. Figure 2.7 displays the O-ring modification used in order to secure the smaller valve in place and the final assembly.

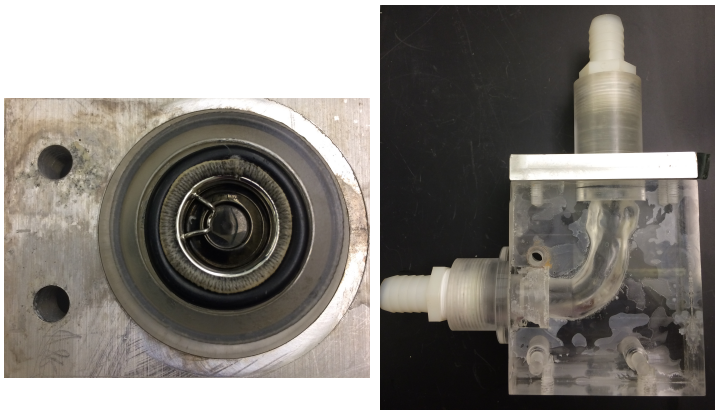

Figure 2.7 (Left): O-Ring Modificaton, (Right): Final Assembly

2.2 Ultrasonic Flow Meter

In order to measure the volumetric flow rate and thus calculate the flow velocity, an ultrasonic flow meter was placed in the loop prior to entrance into the valve holding chamber. The flow meter used in this study was a H20XL-Sterile Tubing Flow Sensor manufactured by Transonic Systems Incorporated (TSI). These flow meters are used in a wide variety of biomedical settings, including artificial heart and VAD performance, medical device testing, and compliance flow testing [36]. These flow meters are capable of measuring volume flow in most non-aerated liquids, including saline, and blood and water buffer solutions without making physical contact to the fluid media [36]. The flow meter functions by clamping around tubing of specific dimension and employing ultrasonic transit time technology to measure the time difference of ultrasonic pulses transmitting both in and against the fluid flow direction [36]. Specifically, four transducers within the sensor pass ultrasonic signals intersecting the fluid path upstream and downstream, and the difference between the four ultrasonic transit times yields a measurement of volume flow at the particular instant in time. Actual volume flow measurements are then digitally displayed in mL or L/min, allowing for continuous monitoring of flow measurements.

The sensor size of the flow meters are determined by outer tubing diameter, with the tubing in this research being 1.25” OD. The sensor size that correlates to this tubing diameter is the H20XL sensor, which has a 50 mL/min resolution, max flow of 100 L/min, and ultrasonic frequency of 1.2 MHz [36]. Resolution is defined as the smallest detectable flow change at 0.1 Hz filter. Prior to clamping the flow meter on the mock loop tubing, a thin layer of petroleum jelly was applied to the section of tubing to serve as an acoustic couplant. This layer enables the ultrasonic transmission between the tube and the sensor. In order to place the flowmeter on the tubing, the lubricated tubing was placed in the sensing cavity and the lid was closed to ensure a tight fit. The tubing cross section was “squared off” with the sensor to ensure contact of all surfaces to the sensing window. Once the tubing was filled with fluid, the flowmeter controls can be operated to measure volume flow. Data collection began after all visible air bubbles were absent from the system.

2.3 Blood Analog Mixture

In order to appropriately assess MHV hemodynamic performance, it is imperative to use a fluid with similar viscous characteristics to human blood. In this study, a mixture of 60% water and 40% glycerin was used as the blood analog. This particular mixture is widely used in various mock loop flow visualization studies, as its properties such as density and viscosity closely match that of natural whole blood. The density of the blood analog results in a value of 1.105 g/mL, whereas the density of natural blood is 1.05 g/mL. The viscosity of the analog has a value of 0.00485 N-s/m^2, whereas natural blood has a viscosity of 0.0027 N-s/m^2. As opposed to whole blood, this mixture presents the advantage of being readily available while not posing safety concerns associated with blood-borne diseases. This mixture also presents a fluid of Newtonian characterization, which is also seen in most arteries. By the definition of a Newtonian fluid, both

the blood analog and whole blood exhibit a linear relationship between shear stress and deformation rate, and its viscosity can be assumed to be a constant value. Approximately 600 mL of water and 400 mL of glycerin was used to fill the loop intended for this particular study. The mixture was prepared in a glass beaker and mixed using a magnetic stirrer prior to implantation into the loop.

2.4 Particle Image Velocimetry (PIV)

In order to visualize the flow across the valve, Particle Image Velocimetry (PIV) was utilized in this research to gain insight on the general flow characteristics of the valve. This technique measures fluid velocity by determining particle displacement over a precisely selected time [33]. A laser light sheet illuminates a plane within the flow, and the positions of the illuminated particles in that plane are recorded using a high speed CCD digital camera. A short duration later, a second image is taken creating a pair of images that can be used to correlate velocity measurements from displacement of the particles. In addition to velocity information, other flow properties such as vorticity, strain rates, turbulence intensity, and general flow structures can be obtained using PIV analysis algorithms embedded in the associated PIV software. Typical PIV systems consist of both hardware and software components, including a laser, synchronizer, CCD camera, and computer with the appropriate software. Figure 2.8 displays the general principle behind typical PIV experimental setup.

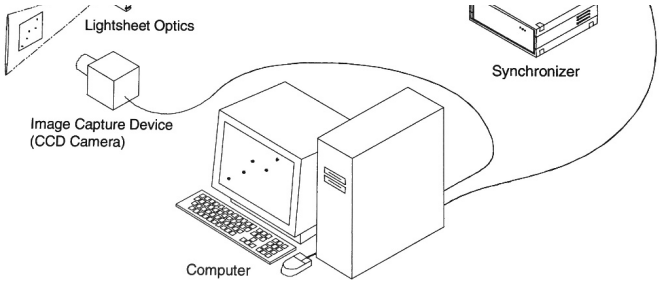

Figure 2.8: Typical PIV Setup [33]

2.4.1 Hardware

2.4.1.1 Camera

In order to capture consecutive images of the fluid path across the valve, a high resolution CCD camera was mounted directly above the valve holding model. The camera was mounted at an optimal distance from the imaging area such that the images provided high contrast and the seeded particles could be visible to the naked eye. The camera is able to capture images of the particles in the fluid path, and digitize the image for further processing on a computer. Specifically, the camera converts light energy into electrical energy, generating an electrical signal that is sent to the Frame Grabber installed in the computer [33]. The CCD camera used in this research was the PIVCAM 10-30 (TSI Incorporated) with a maximum frame rate of 30 Hz, using a CCD array of 1008 x 1018 pixels. The amount of images taken by the camera is controlled using the associated Insight software installed on the computer. The particles used in this research were manufactured by Duke Scientific Corporation, consisting of polymer microspheres spheres with 100 g/mL density and 100-500 μm mean diameter size. These

particles are capable of being illuminated when exposed to laser light sheets, allowing for the camera system to capture their movements within the fluid.

2.4.1.2 Adjustable Laser

The laser light source used in this research was the Altair Series 532nm Green Laser Pointer manufactured by Laserglow Technologies [35]. This particular laser source was chosen due to its capability of adjusting beam width and its wavelength value. By controlling the width of the beam produced by this laser, the flow field surrounding the valve could be properly illuminated. This laser emits a wavelength of 532 mm, which is frequently seen in typical PIV setups. The output power of this laser pointer is 4.0-5.0 mW, has a duty cycle of 90 seconds on and 20 seconds off, and consists of a solid brass casing. This laser was mounted near the valve chamber along with a beam-splitting lens to allow for illumination of the particles within the flow field of interest. The laser light sheet was positioned so that its orientation is at a 90 degree angle to the camera.

2.4.1.3 Computer

The components of the PIV system are controlled and monitored using a Dell Pentium 4 PC with 512 RAM. This particular computer contains a 40 GB hard drive and 1.2 GHz processing speed. This computer is able to communicate with the camera by utilizing the frame grabber installed in the computer. The frame grabber reads the image captured from the camera and displays it as a digital image on the monitor. The digital images are then stored in the RAM and further processed in the associated Insight 3.2 PIV software installed on the computer.

2.4.2 Imaging Software

The software utilized in this research consists of the Insight 3G® global imaging, analysis, and display software produced by TSI. This software is capable of dividing the digital images captured by the camera into designated interrogation areas within the flow field of interest. The typical size of an interrogation region is 32 x 32 pixels, however can be altered within the software [33]. The Insight software allows for the masking of particular regions in the interrogation region, in order to ignore certain unwanted features in the image and reduce noise. After the software divides the images into interrogation regions, it then determines the number of usable particles and their corresponding locations within the two image pairs [33]. Statistical cross-correlation algorithms within the software are used to determine the displacements of the particles and therefore their velocities.

2.5 Research Plan

Through the use of the flow meter and the PIV camera setup, volumetric flow rates and particle images of the valve opening and closing cycles were collected throughout this study. The flow meter was placed on the tubing right before the entrance to the valve holding chamber, allowing volumetric flow rates to be taken at that location throughout the different pump operating conditions. After the flow rates were collected, these values were used to determine average flow velocities at each given operating condition. A sequence of six particle images were captured at each operating condition, to allow for the analysis of local flow behavior during both opening and closing phases of the valve. These images were then post-processed using Matlab® to enhance image contrast to allow for better visual detection of the particles embedded within the flow.

In order to simulate realistic pediatric flow conditions, a specific set of pump operating conditions were selected. Specifically, heart rate (HR) and stroke volume (SV) were varied using adjustable controls present on the Harvard Apparatus Pulsatile blood pump. Conditions for pediatric flow were based on several literature findings [3, 21] and the evidence that increasing heart rate and decreasing stroke volume and cardiac output is expected for younger patients. Heart rates tested ranged from 50-100 strokes/min, with the high-end representing infant patients (1 month- 1 year), and the low-end representing adolescent patients (18+ years). Stroke volume ranged from 15-85 mL/stroke, and systolic duration was kept constant at 30%. The theoretical cardiac output of the pump was calculated and compared to the experimental flow rates the flow meter measured at each operating condition. Table 2.1 displays the pump operating conditions used to simulate pediatric flow used in this study.

Table 2.1: Pump Operating Conditions for Pediatric Flow

Age	**HR (Strokes/Min)**	**Stroke Volume (mL/stroke)**
Adolescent (18+ yrs)	50	85
	60	70
	70	55
Child (5-12 yrs)	80	40
Toddler (1-4 ys)	90	25
Infant (6 months)	100	15

3 RESULTS

The data acquired throughout this study consisted of both flow rate data collected by the flow meter and sequences of PIV images captured by the CCD camera at each operating condition. A total of six unique operating conditions were tested, with varying heart rate and stroke volume combinations. Each operating condition was determined using published pediatric patient flow data, and corresponds to four different pediatric age groups. Systolic duration was kept constant at 30%. The flow rate data was collected using a Transonic flow meter and stored in an Excel file, and then converted to flow velocity values. Flow rate data was initially collected while heart rate was increasing, and subsequently collected as heart rate was decreasing to explore possible hysteresis effects. A set of six sequential PIV images were taken at each operating condition in order to track particle motion throughout opening and closing phases of the valve. The CCD camera used in this study utilized a 28 mm lens with a 30 Hz frame rate, denoting a 33.33 ms time separation between each image capture.

3.1 Flow Rate Data

Table 3.1 displays the average experimental flow rate data (L/min) for each operating condition, with heart rate increasing as data was being collected. The theoretical cardiac output of the pump is also shown and was calculated as heart rate multiplied by stroke volume, and compared to the experimental flow rate values. After collecting average flow rate values, average flow velocity was also determined using the equation $Velocity = \frac{4\times\, flow\ rate}{\pi \times tubing\ diameter}$ where tubing diameter was 1.25 inches. Table 3.2 also displays the experimental flow rate data for each operating condition as heart rate was decreasing.

Table 3.1: Flow Rate Data with Increasing HR

Age	HR (Strokes/Min)	Stroke Volume (mL/stroke)	Cardiac Output (L/min)	Flow Rate (L/min)	Flow Velocity (m/s)
Adolescent (18+ yrs)	50	85	4.25	5.005	1.6
	60	70	4.2	4.96	1.59
	70	55	3.85	4.8	1.54
Child (5-12 yrs)	80	40	3.2	4.45	1.43
Toddler (1-4 ys)	90	25	2.25	3.3	1.06
Infant (6 months)	100	15	1.5	2.45	0.79

Table 3.2: Flow Rate Data with Decreasing HR

Age	HR (Strokes/Min)	Stroke Volume (mL/stroke)	Cardiac Output (L/min)	Flow Rate (L/min)	Flow Velocity (m/s)
Adolescent (18+ yrs)	50	85	4.25	5.145	1.6
	60	70	4.2	5.06	1.59
	70	55	3.85	4.985	1.54
Child (5-12 yrs)	80	40	3.2	4.49	1.43
Toddler (1-4 ys)	90	25	2.25	3.515	1.06
Infant (6 months)	100	15	1.5	2.534	0.79

Figure 3.1 display flow rate versus heart rate for both the theoretical cardiac output of the pump and the experimental flow rate values. For both increasing and decreasing heart rate conditions, experimental flow rate values were higher than theoretical CO calculations at each operating condition. For the increasing heart rate case, the average percent difference between theoretical and experimental values resulted in a value of 34.9%, with the percent difference increasing as heart rate increased. For the decreasing heart rate case, the average percent

difference between theoretical and experimental values resulted in a value of 39.4%, with larger percent differences at higher heart rates as well. This discrepancy between theoretical cardiac output and the measured flow rates are most likely attributed to the Harvard Pump not having a digital read-out as parameters were being adjusted throughout each operating condition.

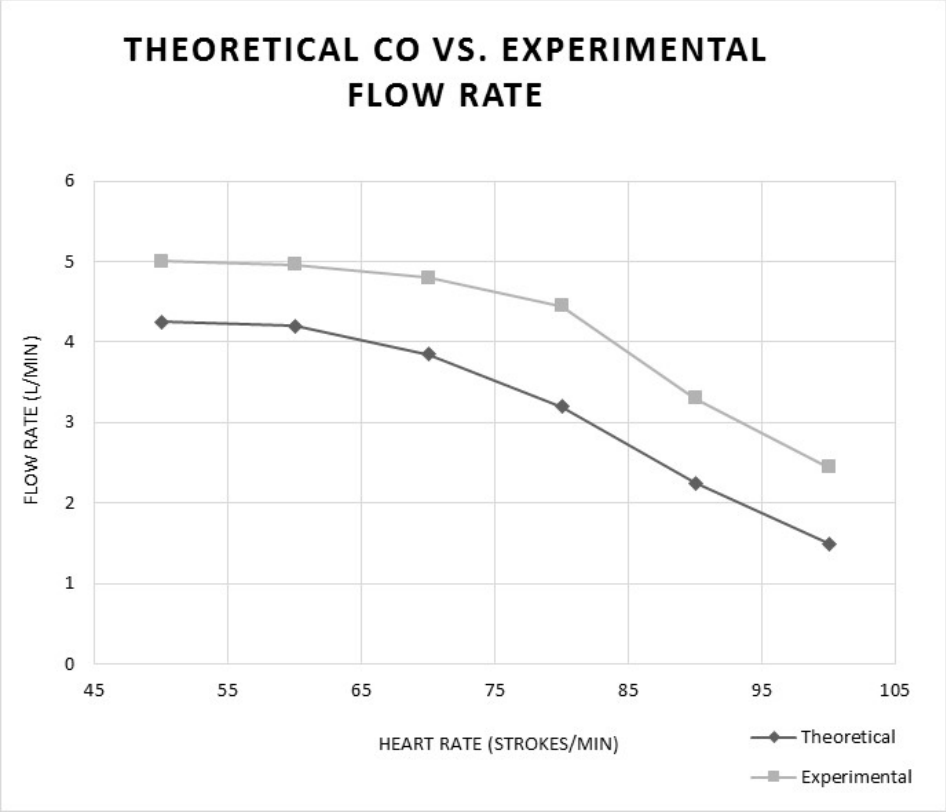

Figure 3.1: Theoretical CO vs. Experimental Flow Rate

3.2 PIV Images

As mentioned previously, six sequential PIV images were captured at each operating condition in order to examine the local flow characteristics of the valve. The camera used operates at a 30 Hz frame rate, denoting a 33.33 ms time separation between each consecutive image. After image capture and storage, Matlab® was used to convert the RGB images to grayscale images and also to enhance contrast. By enhancing the contrast of each image, the

visibility of the illuminated particles was improved. These images were used to make general conclusions of flow characteristics, such as regions of turbulence or recirculation.

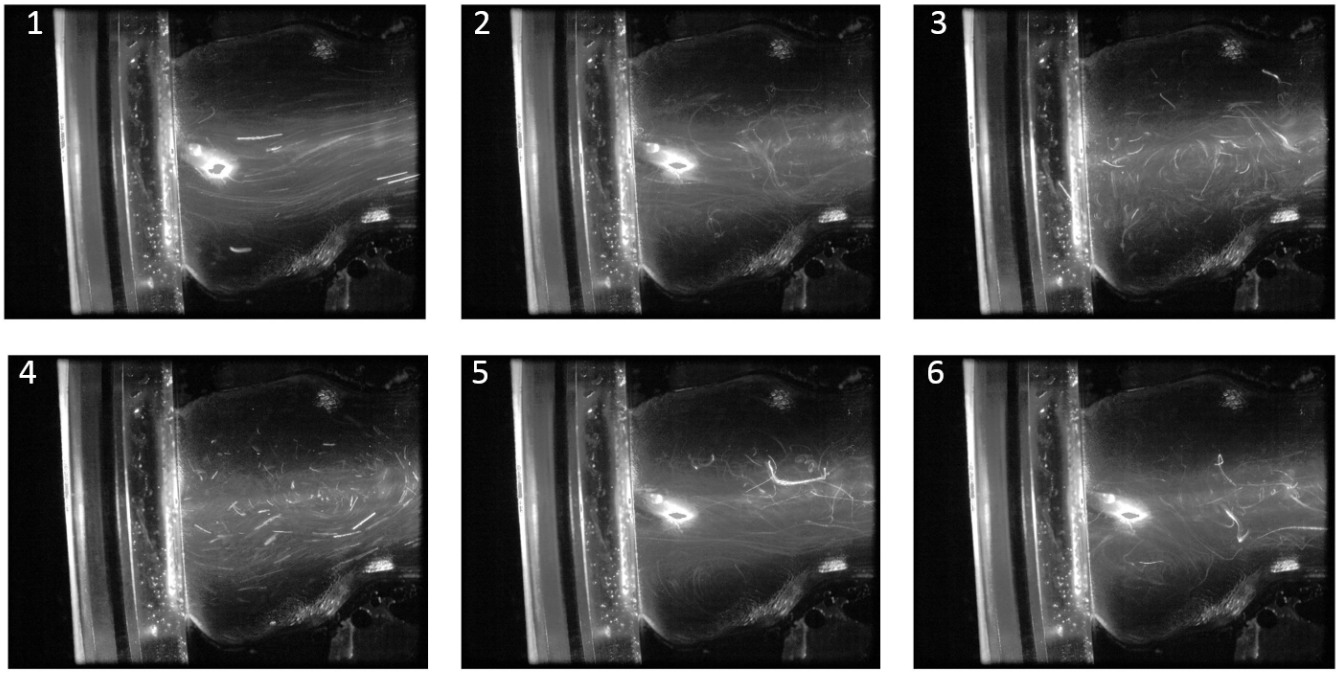

3.2.1 50 BPM at 85 mL Stroke Volume

Figure 3.2: Valve Motion at 50 BPM and 85 mL Stroke Volume

Figure 3.2 shows the six sequential PIV images captured while pump conditions were set to 50 BPM and 85 Stroke volume, with the valve opening 50 times per minute. The flow meter measured an average flow rate of 5.005 L/min during these conditions, with an average flow velocity of 1.6 m/s. Image 1 in the series displays the valve in the fully open position, whereas image 2-4 show the valve entering the closing phase or diastolic phase of the cardiac cycle. Images 5 and 6 show the valve entering the opening phase or systolic phase of the cardiac cycle. Images 2,3, 4 and 6 show evidence of recirculation regions in the local vicinity of the valve.

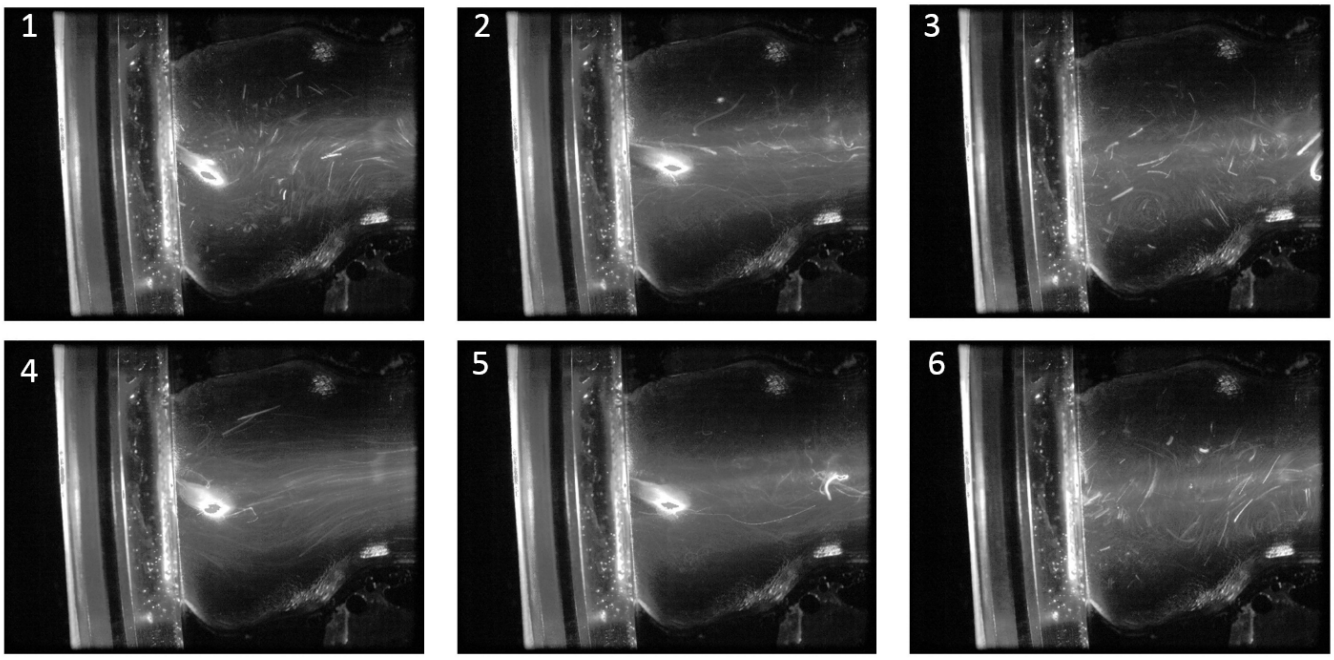

3.2.2 60 BPM at 70 mL Stroke Volume

Figure 3.3: Valve Motion at 60 BPM and 70 mL Stroke Volume

Figure 3.3 shows the six sequential PIV images captured while pump conditions were set to 60 BPM and 70 Stroke volume, with the valve opening 60 times per minute. The flow meter measured an average flow rate of 4.96 L/min during these conditions, with an average flow velocity of 1.59 m/s. Image 1-2 in the series displays the valve entering the open or systolic phase, whereas image 3 show the valve entering the closing phase or diastolic phase of the cardiac cycle.

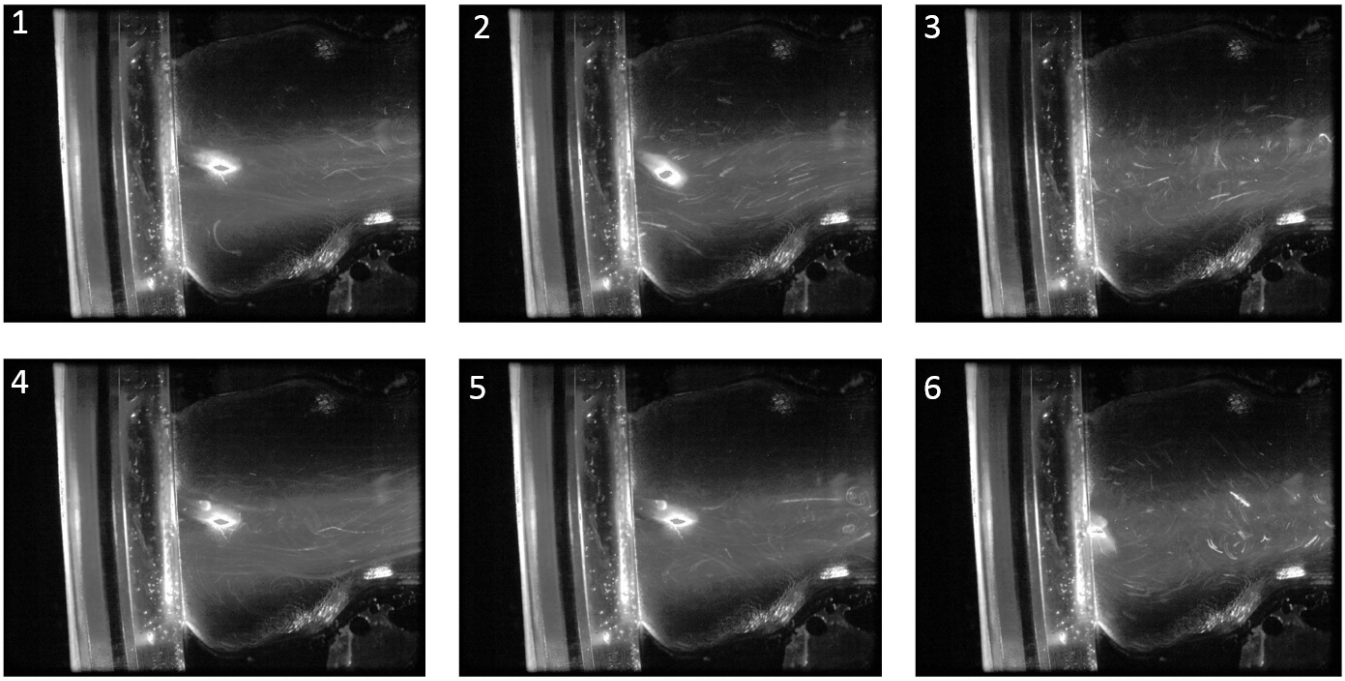

3.2.3 70 BPM at 55 mL Stroke Volume

Figure 3.4: Valve Motion at 70 BPM and 55 mL Stroke Volume

Figure 3.4 shows the six sequential PIV images captured while pump conditions were set to 70 BPM and 55 Stroke volume, with the valve opening 70 times per minute. The flow meter measured an average flow rate of 4.8 L/min during these conditions, with an average flow velocity of 1.54 m/s. Images 1-3 display the valve entering the closing phase or diastolic phase of the cardiac cycle, whereas images 4-5 show the valve during the opening phase.

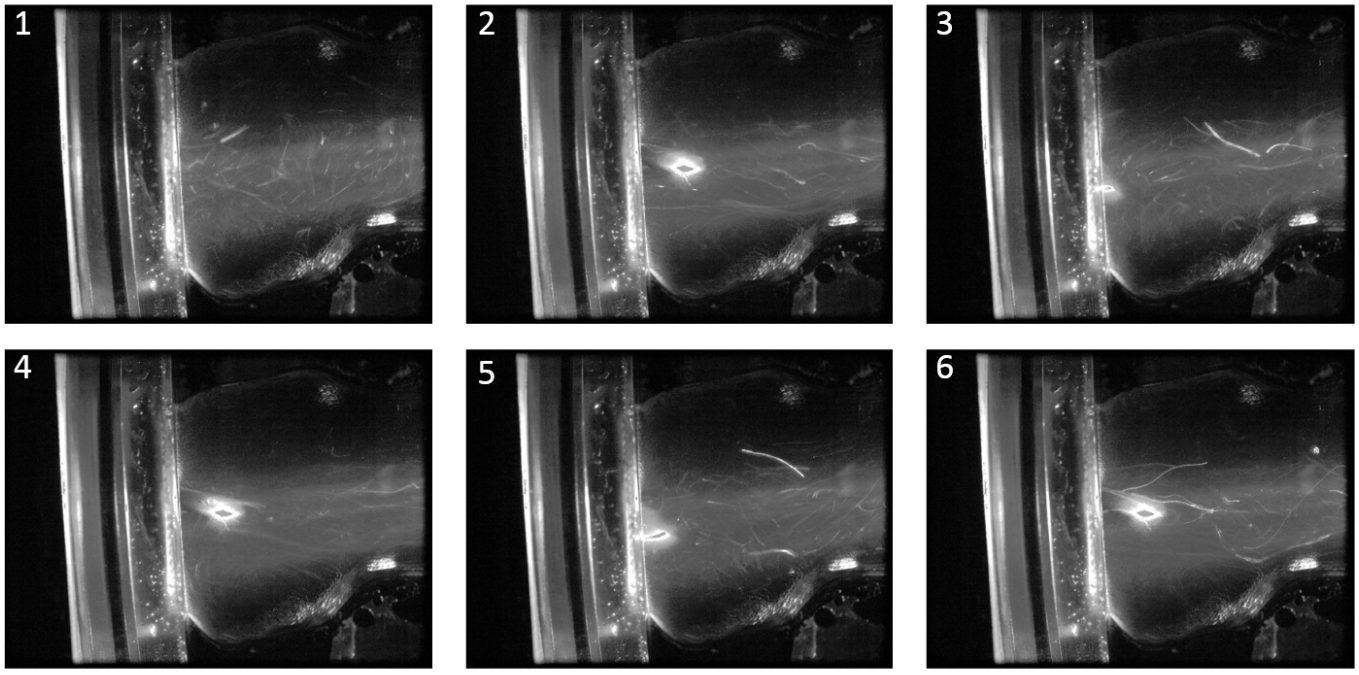

3.2.4 80 BPM at 40 mL Stroke Volume

Figure 3.5: Valve Motion at 80 BPM and 40 mL Stroke Volume

Figure 3.5 shows the six sequential PIV images captured while pump conditions were set to 80 BPM and 40 Stroke volume, with the valve opening 80 times per minute. The flow meter measured an average flow rate of 4.45 L/min during these conditions, with an average flow velocity of 1.43 m/s. Image 1 displays the valve in the closed position, whereas images 2,4, and 6 show the valve entering the opening or systolic phase.

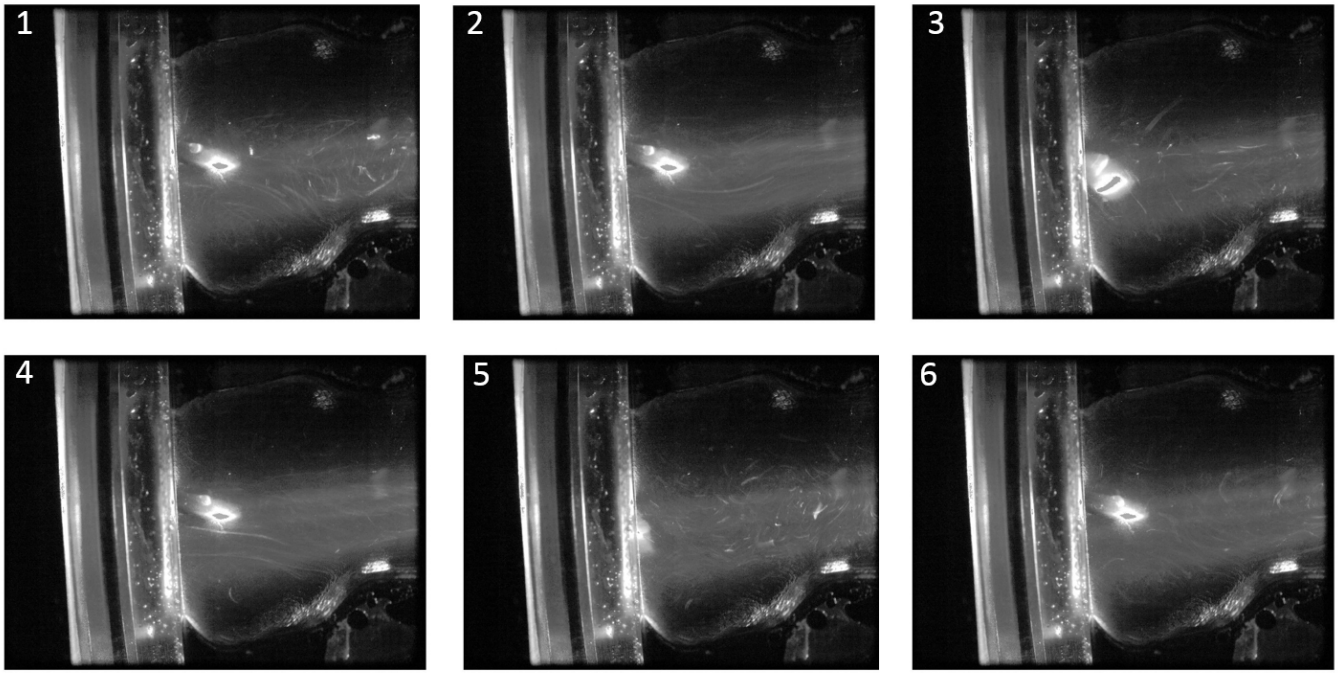

3.2.5 90 BPM at 25 mL Stroke Volume

Figure 3.6: Valve Motion at 90 BPM and 25 mL Stroke Volume

Figure 3.6 shows the six sequential PIV images captured while pump conditions were set to 90 BPM and 25 Stroke volume, with the valve opening 90 times per minute. The flow meter measured an average flow rate of 3.3 L/min during these conditions, with an average flow velocity of 1.06 m/s. Images 1-2 show the valve entering the opening or systolic phase whereas Image 3 show the valve entering the closing phase.

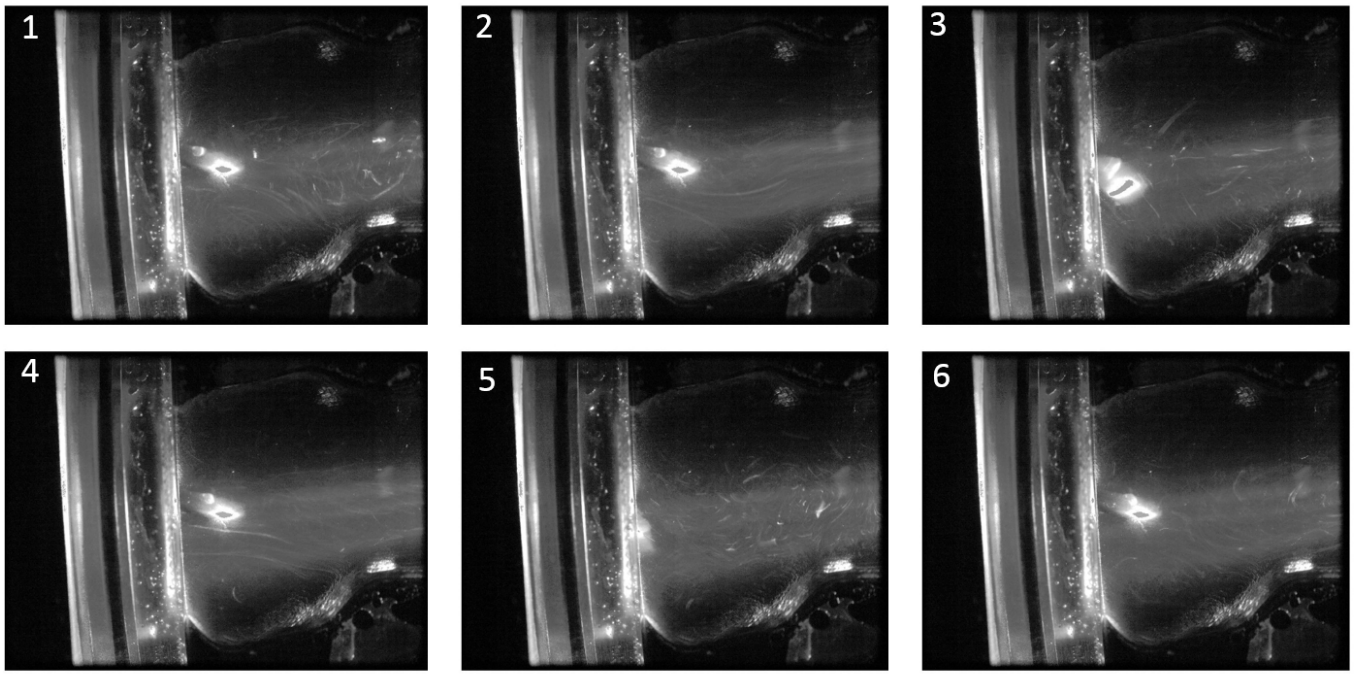

3.2.6 100 BPM at 15 mL Stroke Volume

Figure 3.7: Valve Motion at 100 BPM and 15 mL Stroke Volume

Figure 3.7 shows the six sequential PIV images captured while pump conditions were set to 100 BPM and 15 Stroke volume, with the valve opening 100 times per minute. The flow meter measured an average flow rate of 2.45 L/min during these conditions, with an average flow velocity of 0.79 m/s. Images 1-2 show the valve entering the opening phase, whereas images 3 and 5 show the valve entering closing phase.

4 DICUSSION

This experimental study evaluated the performance of a pediatric-sized tilting disk heart valve under six unique operating conditions, while measuring flow rates and capturing sequential PIV images of the opening and closing phases of the valve. Through the use of the adjustable Harvard Apparatus Pulsatile Blood Pump, six different pediatric flow conditions were tested by altering both heart rate and stroke volume produced by the pump. The six different heart rate and stroke volume combinations were as followed: 1. 50 BPM, 85 mL, 2. 60 BPM, 70 mL, 3. 70 BPM, 55 mL, 4. 80 BPM, 40 mL, 5. 90 BPM, 25 mL, and 6. 100 BPM, 15 mL. These heart rate and stroke volume values were selected in order to accurately simulate heart flow conditions for younger patients. The systolic duration of the pump was kept constant at 30% of the cycle length. The fluid used in this experiment consisted of a water/glycerin mixture, in order to simulate similar fluid properties as whole blood such as viscosity and density. This experiment helps to evaluate and assess the performance of a pediatric sized heart valve within the mock loop experimental set up, which may eventually lead to the progression of knowledge regarding the performance and *in-vitro* testing procedures of pediatric heart valves.

4.1 Flow Rate Data

Through the use of an ultrasonic flow meter, flow rate data was collected prior to the entrance of the heart valve testing chamber. The average flow rates were recorded for each pump operating condition, and used to convert values into average flow velocities. Flow data was recorded for two different scenarios, one being as heart rate was increasing (operating conditions 1 to 6) and one being as heart rate was decreasing (operating conditions 6 to 1). For both cases,

flow rate and thus flow velocities decreased as heart rate increased and stroke volume decreased. This result was anticipated, as younger patients produce lower cardiac outputs due to increased heart rate but decreased stroke volume. This can be explained due to younger myocardium being physiologically different to that of adult or maturing myocardium. Myocardium is the muscle wall of the heart, which is responsible for contracting in order to pump blood out of the heart and relaxing to allow the heart to fill with blood. The myocardium of younger patients, specifically newborns, contains less contractile fibers than that of the adult heart. Due to having less contractile power, younger patients are not able to produce similar cardiac outputs as adults. In addition, adult hearts are able to increase its stroke volume by both strengthening contractions and increasing heart rate. In contrast, the pediatric heart can only increase stroke volume by increasing heart rate. Structurally, children have smaller heart chambers and lower overall blood volume than the adult heart, therefore lower cardiac outputs are expected for younger patients. The flow rate values collected during this study support this, as flow rate consistently decreased with increasing heart rate, as the higher heart rate conditions represent younger patient flow conditions. This flow data also shows the capability of the mock circulatory loop in simulating accurate pediatric flow conditions for the testing of a pediatric sized MHV.

The flow rate data collected during this study was also compared to the theoretical cardiac output of the Harvard pump. For both testing scenarios, the measured flow rates were slightly higher than the associated theoretical cardiac outputs. In addition, the percent difference between measured flow and theoretical output increased significantly as heart rate increased. This difference between measured flow values and the theoretical output of the pump can be attributed to several factors including slight variations of fluid viscosity and density, flow meter sensitivities, and pump inaccuracies. Several times throughout this experiment, small amounts of

water were added to the loop to reduce the presence of air bubbles trapped within the loop. By adding small amounts of water to the loop, the viscosity of the overall water/glycerin mixture may have decreased slightly, resulting in the higher measured flow rates. In addition, flow meter sensitivities may also have contributed to the higher measured flow rate values. Inconsistences such as slight fluctuations in temperature or a non-uniform Vaseline seal between the tubing and the sensor could have attributed to this error. The most significant changes in the uniformity of the ultrasonic beam used in the sensor occur at either the tubing/sensor interface or the tubing/liquid border. In addition, the manual adjustments of the pump for both heart rate and stroke volume do not have digital read-outs, therefore actual pump parameters may have been slightly different from the intended operating condition.

The purpose of collecting data during two different scenarios, one being as heart rate was increasing, and the other being as heart rate was decreasing, was to explore any possible hysteresis effects present within the fluid or equipment. Specifically, the intent was to investigate if the measured flow rates would differ as heart rate was being approached at either the high or low limits. The results indicated that flow rates were not significantly affected as heart rate was being increased or decreased, indicating little hysteresis effects. However, flow rates were slightly higher in the case where heart rate was being decreased from the highest value to the lowest. This may be attributed to the fact that the pump had to go through the lower heart rates prior to reaching the highest value starting point.

4.2 PIV Images

During this study, sequential PIV images were taken at each operating condition to verify proper valve mechanical functionality as well to determine flow characteristics of the opening and closing phases of the valve. In order to visually observe the flow characteristics, particle

illumination and MATLAB post-processing was used in order to increase the contrast between the particles and the background. These images were used to generate qualitative information regarding the structure of the flow, and regions of flow stagnation and recirculation. Such information is useful in the assessment of the valve performance as it relates to clinical complications such as thrombosis and hemolysis.

4.2.1 Opening Phase of Valve (Systole)

During the opening phase of the valve, the images collected display certain flow characteristics that are typical of a tilting disc valve, such as producing a major and minor outflow region. The major and minor flow regions are produced by the 60 degree tilt of the disc when in the fully opened position during systole. The major outflow jet is characterized by being larger spatially and well as appearing to have higher local velocity, and thus likely producing higher shear stresses in this region. The minor outflow region is smaller, with lower local velocities and likely more dispersed stresses.

As heart rate increases and stroke volume decreases, average flow velocities during the open phase of the valve decrease. Specifically, flow velocities of approximately 1.6 m/s were achieved during the first operating condition (50 BPM, 85 mL), whereas flow velocities as low as 0.79 m/s were recorded during the last operating condition (100 BPM, 15 mL). This is visually evident in the images captured during the opening phases of the valves at each condition by examining the particle motion. Specifically, lower heart rates showed more streamlined, laminar flow and higher heart rates showed more disorganized, random forward flow during the open phase. This may be attributed to the higher heart rate conditions having less time for the fluid flow to fully develop, as well as the decreased stroke volume per beat. The disorganized,

slower forward flow seen with the higher heart rate conditions may lead to regions of potential flow stagnation under such flow conditions.

4.2.2 Closing Phase of Valve (Diastole)

Certain flow characteristics during the closing phase of the valve were also evident in the sequences of PIV images collected. For instance, a small degree of retrograde flow can be seen in the images just before valve closure. These instances of retrograde flow coincide with the Harvard pump's diastolic phase, which is dominated by the motor's drawback mechanisms. Regions of regurgitant and swirling flow are also evident throughout the valve's closing phase during each operating condition, specifically right after valve closure. By examining the images at each operating condition, these regions of swirling regurgitant flow seem to dissipate as heart rate increased. This may be attributed to the higher heart rate conditions having less time spent in the diastolic or drawback phase of the Harvard pump. With less time spent in the diastolic phase, less backflow can occur and the magnitude of the swirling regions seems to decrease. The largest amount of recirculating, swirling flow occurs when the operating conditions were set to 50 BPM and 85 mL stroke volume, whereas the least amount of swirling occurring at 100 BPM and 15 mL. This suggests that heart rate has a significant effect on regurgitant volume during the closing phase of a pediatric sized tilting disc valve.

The location and structure of the swirling flow regions varies throughout the different operating conditions tested. The two operating conditions that displayed the most prominent amount of recirculation during the closing phase were the two conditions with the lowest heart rates; 50 BPM and 85 mL stroke volume and 60 BPM and 70 mL stroke volume. The operating condition with 50 BPM and 85 mL stroke volume appeared to develop a region of recirculation in the major orifice region near the edge of the leaflet at the beginning of valve closure. After

complete valve closure, the swirling region appears to travel downstream the valve, growing larger and translating more to the mid-line of the fluid path. This may be attributed to the valve holding chamber producing minimal compliance at the time of occluder impact, accentuating recirculation in the local vicinity of the valve. Figure 4.1 displays two images captured during the closing phase at the 50 BPM and 85 mL operating condition, with the circled regions being were the most prominent recirculating regions occur.

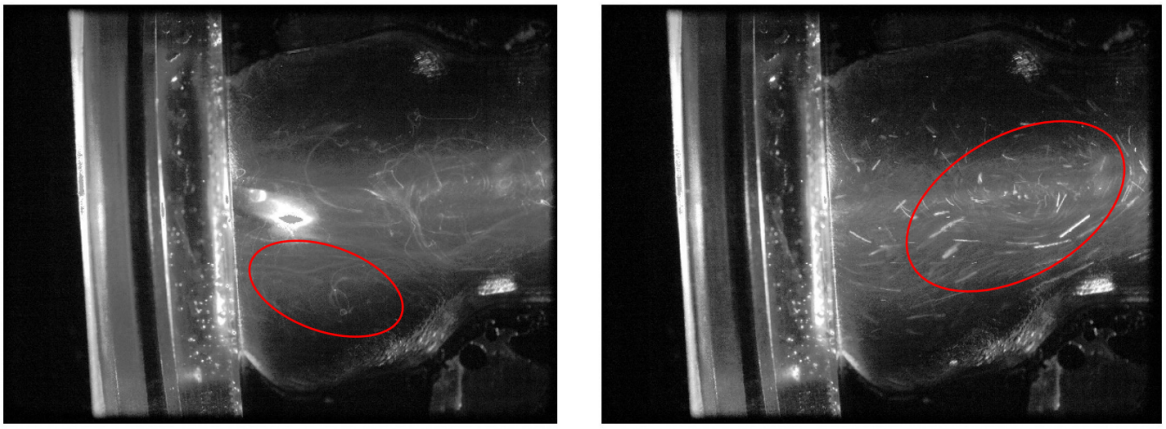

Figure 4.1: Regions of Recirculation with 50 BPM and 85 mL SV

The operating condition with the second lowest HR (60 BPM and 70 mL) also displayed regions of recirculation during the valve closing phase. However this set of images showed a recirculating region appearing in the minor orifice region at the tip of the valve leaflet during valve closure. This recirculating region at the tip of the leaflet may lead to the development of a vortex structure, which makes this region susceptible to potential cavitation. Once the valve was fully closed, recirculation regions were apparent in the lower bulging sinus region of the valve testing chamber. Pockets of recirculating flow in this bulging sinus region can be attributed to this region acting as a reservoir-type structure during the diastolic phase of the Harvard pump. Figure 4.2 displays these regions of recirculation during valve closure at 60 BPM and 70 mL.

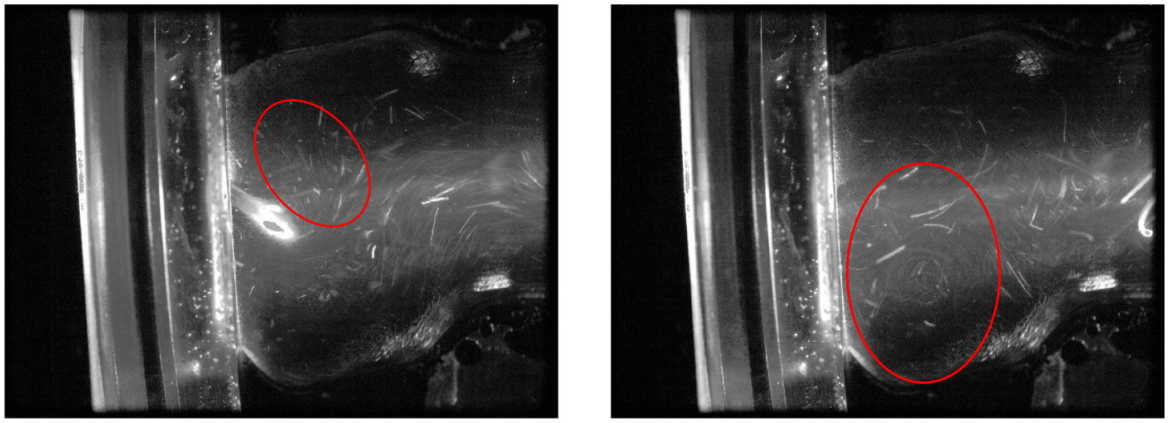

Figure 4.2: Regions of Recirculation at 60 BPM and 70 mL SV

As mentioned previously, these images suggest more swirling regions occur during valve closure in the lower heart rate cases, the operating conditions intended to simulate older patient flow conditions. This suggests that as the patient ages, these regurgitant regions may lead to clinical complications such as thrombotic or hemolytic activity. Although significant regurgitant or swirling regions may have adverse long term effects, a small degree of retrograde flow in tilting disc valves is advantageous and expected. This small degree of retrograde flow is capable of producing a washout effect between the disc and the housing of the valve, washing away any thrombus formations.

Possible Future Progression

The Artificial Heart Laboratory at Virginia Commonwealth University is constantly seeking to make improvements and advancements in mock circulatory loop testing in regards to mechanical heart valve evaluation. Possible future progression in terms of mock loop testing may include the incorporation of additional loop components to provide a more accurate physiological environment. Such components may include variable resistors to simulate arterial and peripheral resistance, as well as additional capacitors to simulate ventricular compliance.

Such components were excluded in this research because the primary focus of this study was the investigation of local valve fluid behavior, with less emphasis on mock loop performance. Such mock loop improvements will further expand the scope of mechanical heart valve testing in the future.

In addition, the testing and evaluating of different pediatric valves could provide a larger breadth of knowledge regarding the performance of pediatric valves in experimental settings. As an example, the testing of a pediatric-sized bileaflet valve would allow for the comparison between bileaflet and tilting disc valve performance. The testing of a variety of different sized pediatric valves would also be beneficial as it would allow for the comparison of flow behavior across a multitude of valve sizes. A heart valve testing chamber capable of holding a range of valve sizes could facilitate such testing in the future. By doing so, more conclusive data could be collected regarding the performance of pediatric valves under experimental conditions.

Conclusions

With congenital heart valve disease being among one of the most common heart defects found in the pediatric population, the testing and evaluation of pediatric sized mechanical heart valves is imperative to the development of such valves. As there are currently no FDA approved mechanical heart valves available for the use in pediatric patients, it is necessary to develop standard *in-vitro* testing procedures in order to gain a better understanding of the fluid mechanics associated with smaller sized heart valves. The research presented here describes the development of an *in-vitro* experimental set-up that is capable of evaluating the functionality of a pediatric-sized tilting disc valve, a common valve chosen for implantation in pediatric patients. The experimentation involved the incorporation of a mechanical heart valve testing chamber into a mock circulatory loop that is capable of simulating a wide range of cardiovascular

physiological conditions. Specifically, the Harvard Apparatus Pulsatile pump was used in this research to simulate pre-determined pediatric flow conditions, by altering both the heart rate and stroke volume produced by the pump. A set of six unique pump operating conditions were chosen to model pediatric flow, ranging from 6 months of age to 18+ years. Through the use of fluid flow visualization techniques and flow rate measurement, specific flow characteristics were observed during both the opening and closing phases of the valve. The results from this study indicated a decrease in flow rate and velocity as heart rate was increased, which is expected in younger patients. In addition, the lower heart rate conditions displayed more of a streamlined, laminar flow during the open phase, whereas the higher heart rates displayed a more disorganized, random forward flow. During the closing phase of the valve, more regions of recirculating, swirling flow were seen in the lower heart rate conditions. Specifically, the major regions of recirculation included the regions surrounding the tip of the valve leaflet. These regions of swirling flow may lead to the development of potential clinical complications such as thrombosis and cavitation. By characterizing the general flow behavior of this pediatric-sized mechanical heart valve, this study may aide in the design and development of additional mechanical heart valves intended for the pediatric population. Localized design changes such as altering the shape of the leaflet edge, may contribute to more positive fluid mechanics behavior specifically during valve closure.

REFERENCES

1. Yoganathan, A., He, Z., & Jones, C. (2004). Fluid Mechanics of Heart Valves. *Annu. Rev. Biomed. Eng, 6*, 331-62. Retrieved from http://www.ncbi.nlm.nih.gov/pubmed/15255773
2. Yoganathan, A., Fogel, M., Gamble, S., Morton, M., Schmidt, P., Secunda, J., . . . Nido, P. (2013). A new paradigm for obtaining marketing approval for pediatric-sized prosthetic heart valves. *The Journal of Thoracic and Cardiovascular Surgery,* 879-886.
3. Yun, B., McElhinney, D., Mirabella, L., Aidun, C., & Yoganathan, A. (2014). Computational simulations of flow dynamics and blood damage through a bileaflet mechanical heart valve scaled to pediatric size and flow. *Journal of Biomechanics,* 3169-77.
4. Anatomy of the Heart. (n.d.). Retrieved October 1, 2015, from http://www.nhlbi.nih.gov/health/health-topics/topics/hhw/anatomy
5. Aortic Valve Stenosis. (n.d.). Retrieved October 1, 2015, from http://pediatricheartspecialists.com/articles/detail/aortic_valve_stenosis
6. How Is Heart Valve Disease Treated? (n.d.). Retrieved October 1, 2015, from http://www.nhlbi.nih.gov/health/health-topics/topics/hvd/treatment
7. Laudito, A., Brook, M., Suleman, S., Bleiweis, M., & Thompson, L. (2000). The Ross Procedure in Children and Young Adults: A word of caution. *The Journal of Thoracic and Cardiovascular Surgery, 122*(1).
8. Kadner, A., Raisky, O., Degandt, A., Tamisier, D., Bonnet, D., Sidi, D., & Vouhé, P. (n.d.). The Ross Procedure in Infants and Young Children. *The Annals of Thoracic Surgery,* 803-808.
9. Alsoufi, B. (2014). Aortic valve replacement in children: Options and outcomes. *Journal of the Saudi Heart Association, 26*(1), 33-41.
10. Suzuki, I., Shiraishi, Y., & Yabe, S. (n.d.). Engineering analysis of the effects of bulging sinuses in a newly designed pediatric pulmonary heart valve on hemodynamic function. *Journal of Artifical Organs,* 49-56.
11. Raghuveer, G., Caldarone, C., & Hills, C. (2003). Predictors of Prosthesis Survival, Growth, and Functional Status Following Mechanical Mitral Valve Replacement in Children Aged. *Surgery for Congenital Heart Disease*.
12. Congenital Heart Center. (n.d.). Retrieved October 1, 2015, from http://www.mottchildren.org/medical-services/ped-heart/conditions/aortic-stenosis
13. Moore, P., Adatia, I., Spevak, P., Keane, J., Perry, S., Castaneda, A., & Lock, J. (1994). Severe congenital mitral stenosis in infants. *Circulation,* 2099-2106.

14. Aortic regurgitation in children. (n.d.). Retrieved October 1, 2015, from http://www.uptodate.com/contents/aortic-regurgitation-in-children
15. Gott, V., Alejo, D., & Cameron, D. (2003). Mechanical Heart Valves: 50 Years of Evolution. *The Annals of Thoracic Surgery, 76*, 2230-2239. Retrieved from http://www.annalsthoracicsurgery.org/article/S0003-4975(03)01815-0/pdf
16. Brown, C., Leverett, L., & Lewis, C. (1975). Morphological, biochemical, and functional changes in human platelets subjected to shear stress. *J Lab Clin Med,* 462-71.
17. Chandran, K., Cabell, G., Khalighi, B., & Chen, C. (n.d.). Laser anemometry measurements of pulsatile flow past aortic valve prostheses. *Journal of Biomechanics,* 865-873.
18. Yoganathan, A., Woo, Y., & Sung, H. (1986). Turbulent shear stress measurements in the vicinity of aortic heart valve prostheses. *Journal of Biomechanics,* 433-442.
19. Fontaine, A., He, S., Ellis, J., Levine, R., & Yoganathan, A. (1996). In vitro assessment of prosthetic valve function in mitral valve replacement with chordal preservation techniques. *Journal Heart Valve Disease*.
20. Meyer, R., Deutsch, S., Bachmann, C., & Tarbell, J. (2001). Laser Doppler velocimetry and flow visualization studies in the regurgitant leakage flow region of three mechanical mitral valves. *Journal of Artifical Organs*.
21. Zapanta, C., Liszka, E., Stinebring, D., Deutsch, S., Geselowitz, D., & Tarbell, J. (1994). Real-time in vitro observation of cavitation on prosthetic heart valves. *1993 IEEE Annual Northeast Bioengineering Conference*.
22. Yoganathan, A., Chandran, K., & Sotiropoulos, F. (2005). Flow in prosthetic heart valves: State-of-the-art and future directions. *Ann Biomed Eng*.
23. Browne, P., Ramuzat, A., Saxena, R., & Ajit P. Yoganathan 1@affil = Cardiovascular. (2000). Experimental Investigation of the Steady Flow Downstream of the St. Jude Bileaflet Heart Valve: A Comparison Between Laser Doppler Velocimetry and Particle Image Velocimetry Techniques. *Annals of Biomedical Engineering, 28*(1), 39-47.
24. Manning, K. B., Kini, V., Fontaine, A. A., Deutsch, S., & Tarbell, J. M. (2003). Regurgitant Flow Field Characteristics of the St. Jude Bileaflet Mechanical Heart Valve under Physiologic Pulsatile Flow Using Particle Image Velocimetry. *Artificial Organs, 27*(9), 840-846.
25. Manning, K. B., Przybysz, T. M., Fontaine, A. A., Tarbell, J. M., & Deutsch, S. (2005). Near Field Flow Characteristics of the Bjork-Shiley Monostrut Valve in a Modified Single Shot Valve Chamber. *ASAIO Journal, 51*(2), 133-138.

26. Pantalos, G. M., Koenig, S. C., Gillars, K. J., Giridharan, G. A., & Ewert, D. L. (2004). Characterization of an Adult Mock Circulation for Testing Cardiac Support Devices. *ASAIO Journal, 50*(1), 37-46.
27. Bjork, V. O., Intonti, F., & Meissl, A. (1962). A Mechanical Pulse Duplicator for Testing Prosthetic Mitral and Aortic Valves. *Thorax, 17*(3), 280-283.
28. Rosenberg, G., Winfred M. Phillips, Donald L. Landis, and W.S. Pierce. (1981). "Design and evaluation of the Pennslyvania State University Mock Circulatory System", ASAIO J, 4, 2, 41-49.
29. Pediatric Mitral Valve Insufficiency. (n.d.). Retrieved March 02, 2016, from http://emedicine.medscape.com/article/890315-overview#a6
30. Taylor, C. (2009). Automated mock loop designed for left ventricular assist device testing. Poster presented at SEBCC 2009.
31. Taylor C.E., Kelly G.S., Miller G.E. Poster presentation at the 2011 annual meeting of the Biomedical Engineering Society; Hartford, CT. "A novel tracing method applied to Visible Human Project cryo slice data to build an aortic model." October 12, 2011
32. Harvard Apparatus Series 1400 Pulsatile Blood Pump User's Manual
33. TSI Particle Image Velocimetry Hardware Operations Manual and INSIGHT Software Version 3.2 Quick Start Guide.
34. Lukic, B., Zapanta, C. M., Griffith, K. A., & Weiss, W. J. (2005). Effect of the Diastolic and Systolic Duration on Valve Cavitation in a Pediatric Pulsatile Ventricular Assist Device. *ASAIO Journal, 51*(5), 546-550.
35. Laserglow Technologies. (n.d.). Retrieved April 07, 2016, from https://www.laserglow.com/GAL
36. Verify Flow Over Wide Dynamic Range with Non-Invasive Sensor: Transonic Flow Meter. (n.d.). Retrieved from http://www.transonic.com/default/assets/File/HT110 Bypass Flowmeter Literature Pack (EC-100-lit-A4)(2).pdf

APPENDIX

MATLAB Code used to increase contrast of PIV images:

```
>> RGB1= imread ('con61.jpg');
A = rgb2gray(RGB1);
A_imadjust=imadjust(A);
RGB2= imread ('con62.jpg');
B = rgb2gray(RGB2);
B_imadjust=imadjust(B);
RGB3= imread ('con63.jpg');
C = rgb2gray(RGB3);
C_imadjust=imadjust(C);
RGB4= imread ('con64.jpg');
D = rgb2gray(RGB4);
D_imadjust=imadjust(D);
RGB5= imread ('con65.jpg');
E = rgb2gray(RGB5);
E_imadjust=imadjust(E);
RGB6= imread ('con66.jpg');
F = rgb2gray(RGB6);
F_imadjust = imadjust(F);
figure,imshow(A_imadjust)
Figure, imshow (B_imadjust)
Figure, imshow (C_imadjust)
Figure, imshow (D_imadjust)
Figure, imshow (E_imadjust)
Figure, imshow (F_imadjust)

>>  % Code used to increase contrast of PIV Images
```

VITA

Sarah Brady Lederer was born October 19th, 1992 in Annapolis, Maryland. She graduated from East Carolina University with a Bachelor's of Science in General engineering in 2014. Upon graduation, Sarah entered the Biomedical Engineering graduate program at Virginia Commonwealth University to pursue her Master's degree. Sarah began working in the Artificial Heart Laboratory under the supervision of Dr. Gerald Miller in December 2014. Sarah plans for relocate to North Carolina upon graduation and begin her career as an engineer.